This research has been co-financed by the European Union (European Social Fund, ESF) and Greek national funds through the Operational Program "Education and Lifelong Learning" of the National Strategic Reference Framework (NSRF), under the grants schemes "Funding of proposals that have received a positive evaluation in the 3rd and 4th Call of ERC Grant Schemes"

The Holographic Way: String Theory, Gauge Theory and Black Holes
Nordita, 15 October 2012

Holographic models for QCD in the Veneziano limit

Elias Kiritsis

University of Crete APC, Paris

Bibliography

Based on work with:

Matti Jarvinnen (Crete) arXiv:1112.1261 [hep-ph]

and ongoing work with:

- T. Alho (Helsinki), M. Jarvinnen (Crete), K. Kajantie (Helsinki), K. Tuominnen (Helsinki).

- D. Arean (SISSA) I. Iatrakis, (Crete), M. Jarvinnen (Crete)

Introduction

• For several phenomena in QCD the presence of quarks is important ($SU(N_c)$ theory with N_f quarks).

• Sometimes the relevant physics can be studied in the "Quenched Approximation": quarks are probes in the glue dynamics.

• For others however, one should include propagating quarks inducing quantum corrections in order to see them. In this second class we can mention:

♠ The conformal window: the theory flows to an IR CFT for $x \equiv \frac{N_f}{N_c} \geq x_c$ if quarks are massless. Chiral symmetry is expected to remain unbroken in this phase. The conformal window ends at the Banks-Zaks point, $x = \frac{11}{2}$.

♠ The phase transition at $x = x_c$ that is conjectured to be in the BKT class. This type of transition where for $x < x_c$ there is a condensate is known as a conformal transition.

Miransky, Kaplan+Stephanov+Son

♠ The region just below x_c where the theory is expected to exhibit walking behavior. This type of behavior is useful for technicolor models.

♠ The QCD thermodynamics as a function of x.

♠ The phase diagram as a function of baryon density. Here we expect a color superconducting phase, as well as a color-flavor locking phase.

Alford+Rajagopal+Wilczek

• All of the phenomena above except the Banks-Zaks region are at strong coupling and therefore hard to analyze.

• Several (uncontrolable) techniques were applies so far for their study: Truncated Schwinger-Dyson equations, lattice calculations, guesswork on β functions, etc. It is with such techniques that some of the expectations above were found.

• The purpose of our effort is to explore the construction of holographic models that exhibit similar phenomena, so that: (a) Explore the landscape of possibilities (b) Construct realistic strong coupling models of QCD in the Veneziano Limit.

The Veneziano limit

- The 't Hooft limit

$$N_c \to \infty, \qquad \lambda = g^2_{\rm YM} N_c \to \text{fixed}$$

always samples the quenched approximation as N_f is kept fixed as $N_c \to \infty$.

- The proper limit in order to study the previous phenomena in the large N_c approximation is the limit introduced by Veneziano in (1976)

$$N_c \to \infty \quad , \quad N_f \to \infty \quad , \quad \frac{N_f}{N_c} = x_f \to \text{fixed} \quad , \quad \lambda = g^2_{\rm YM} N_c \to \text{fixed}$$

- In terms of the dual string theory, the boundaries of diagrams are not suppressed anymore: surfaces with an arbitrary number of boundaries contribute at the same order (for the flavor singlet sector).

The Banks-Zaks region

- The QCD β function in the V-limit is

$$\dot{\lambda} = \beta(\lambda) = -b_0\lambda^2 + b_1\lambda^3 + \mathcal{O}(\lambda^4) \ , \ b_0 = \frac{2}{3}\frac{(11-2x_f)}{(4\pi)^2} \ , \ b_1 = -\frac{2}{3}\frac{(34-13x_f)}{(4\pi)^4}$$

- The Banks-Zaks region is

$$x_f = \frac{11}{2} - \epsilon \quad with \quad 0 < \epsilon \ll 1$$

We obtain a fixed point of the β-function at

$$\lambda_* \simeq \frac{(8\pi)^2}{75}\epsilon + \mathcal{O}(\epsilon^2)$$

which is trustable in perturbation theory, as λ_* can be made arbitrarily small.

• The mass operator, $\bar{\psi}_L \psi_R$ has now dimension smaller than three, from the perturbative anomalous dimension (in the V-limit)

$$-\frac{d\log m}{d\log \mu} \equiv \gamma = \frac{3}{(4\pi)^2}\lambda + \frac{(203 - 10x_f)}{12\,(4\pi)^4}\lambda^2 + \mathcal{O}(\lambda^3, N_c^{-2})$$

• Extrapolating to lower x we expect the phase diagram

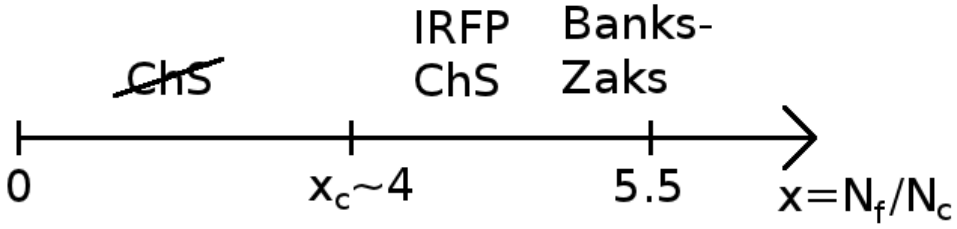

Walking, Technicolor, S-parameter, dilatons

• Walking dynamics has been advocated as a necessary practical ingredient for technicolor models. This has been associated to a large anomalous dimension for the quark mass operator.

Holdom, Appelquist+Karabali+Wijewardhana

• It has been suggested that the S-parameter might be small in the walking region.

Appelquist+Sannino

• It has also been conjectured that there is a special scalar state that is hierarchically lighter than the rest in the walking region, (the "dilaton") reflecting the nearly broken scale invariance.

Yamawaki+Bando+Matumoto

• Such properties have oscillated between fact and fancy in the past 30 years. Their status has not been decided yet.

The strategy

- Construct a (toy) holographic model for QCD in the Veneziano limit.

- Put together two ingredients: the holographic model for glue developped earlier: IHQCD

Gursoy+E.K+Nitti

- and the model for flavor based in Sen's tachyon action.

Casero+E.K.+Paredes, Iatrakis+E.K.+Paredes

The holographic models: glue

For YM, ihQCD is a well-tested holographic, string-inspired bottom-up model with action

Gursoy+Kiritsis+Nitti, Gubser+Nelore

$$\mathcal{S}_{\rm g} = M^3 N_c^2 \int d^5x \sqrt{g} \left[R - \frac{4}{3}(\partial\phi)^2 + V_g(\phi) \right]$$

and Poincaré-invariant metric

$$ds^2 = e^{2A(r)}(dr^2 + \eta_{\mu\nu} dx^\mu dx^\nu)$$

- The potential V_g $\leftrightarrow$ QCD β-function
- the "scale factor" A $\leftrightarrow$ $\log \mu$ energy scale.
- e^ϕ $\leftrightarrow$ λ 't Hooft coupling

In the UV $\lambda \to 0$ and

$$V_g = V_0 + V_1\lambda + V_2\lambda^2 + \mathcal{O}(\lambda^3)$$

In the IR $\lambda \to \infty$ and

$$V_g \sim \lambda^{\frac{4}{3}}\sqrt{\log\lambda} + \cdots$$

• With an appropriate tuning of two parameters in V_g the model describes well both $T = 0$ properties as well as thermodynamics.

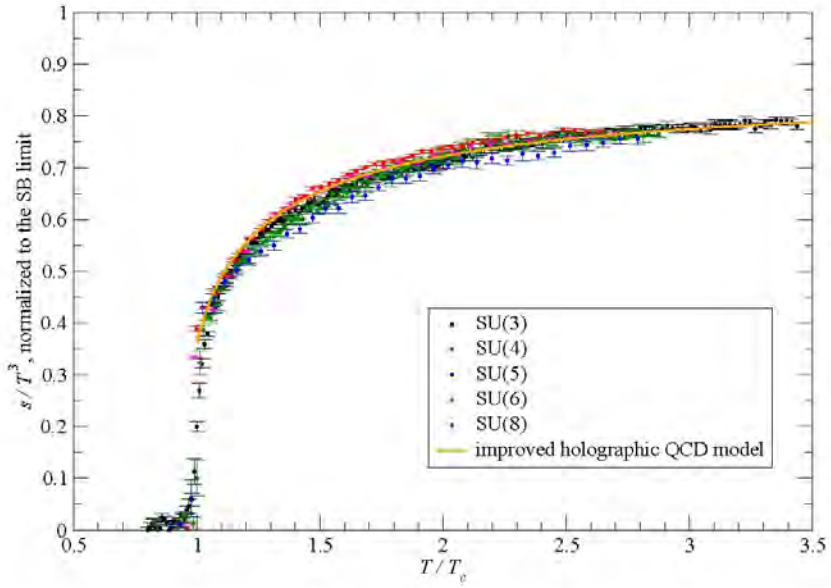

Figure 4: (Color online) Same as in fig. 1, but for the s/T^3 ratio, normalized to the SB limit.

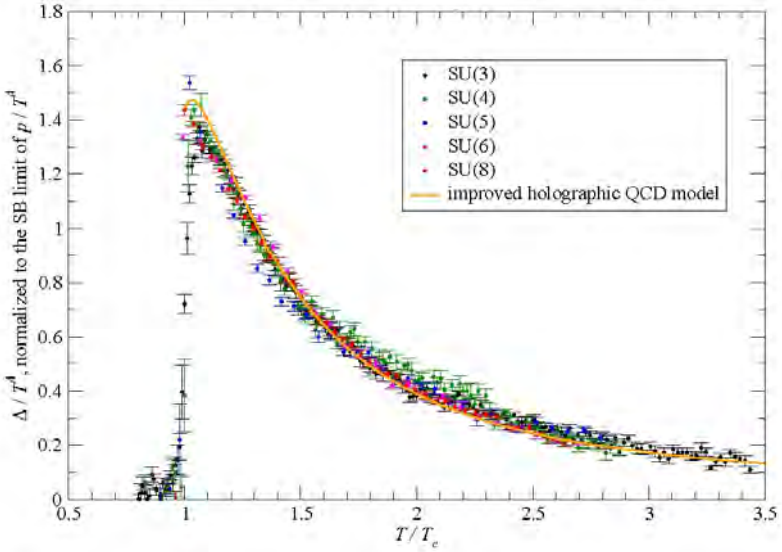

Figure 2: (Color online) Same as in fig. 1, but for the Δ/T^4 ratio, normalized to the SB limit p/T^4.

Panero

The holographic models: flavor

- Fundamental quarks $\rightarrow$ probe D_4-$\bar{D}_4$ branes in 5-dimensions.

$$q_L \quad \leftrightarrow \quad D_3 - D_4 \quad , \quad q_R \quad \leftrightarrow \quad D_3 - \overline{D}_4$$

- We have the gauge fields

$$D_4 - D_4 \quad \rightarrow \quad A_L^\mu \quad \leftrightarrow \quad J_L^\mu \simeq \bar{\psi}_L^i \gamma^\mu \psi_L^j \quad , \quad \overline{D_4} - \overline{D_4} \quad \rightarrow \quad A_R^\mu \quad \leftrightarrow \quad J_R^\mu \simeq \bar{\psi}_R^i \gamma^\mu \psi_R^j$$

and a bifundamental scalar, the "tachyon"

$$D_4 - \overline{D_4} \quad \rightarrow \quad T_{ij} \quad \leftrightarrow \quad \bar{\psi}_L^i \psi_R^j$$

- For the vacuum structure only the tachyon is relevant. It is expected that its backreaction on glue will be crucial in shaping the phase diagram,

Klebanov+Maldacena, Bigazzi+Casero+Cotrone+Kiritsis+Paredes

- An action for the tachyon motivated by the Sen action has been advocated as the proper dynamics of the chiral, condensate giving in general all the expected features of χSB.

Casero+Kiritsis+Paredes

$$\mathcal{S}_{\text{TDBI}} = -N_f N_c M^3 \int d^5x \; V_f(T) \; e^{-\phi} \sqrt{-\det(g_{ab} + \partial_a T \partial_b T)}$$

Fusion

The idea is to put together the two ingredients in order to study the chiral dynamics and its backreaction to glue.

$$\mathcal{S} = N_c^2\ M^3 \int d^5x\sqrt{g}\left[R - \frac{4}{3}\frac{(\partial\lambda)^2}{\lambda^2} + V_g(\lambda)\right] -$$

$$-N_f N_c\ M^3 \int d^5x V_f(\lambda,T)\sqrt{-\det(g_{ab}+h(\lambda)\partial_a T\partial_b T)}$$

with

$$V_f(\lambda,T) = V_0(\lambda)\ \exp(-a(\lambda)T^2)$$

- We must choose $V_0(\lambda), a(\lambda), h(\lambda)$.

♠ The simplest and most reasonable choices, compatible with glue dynamics do the job! The phase structure at $T=0$ is robust against many different choices in the IR.

Parameters

• A theory with a single relevant (or marginally relevant) coupling like YM has no parameters.

• The same applies to QCD with massless quarks.

• QCD with all quarks having mass m has a single (dimensionless) parameter : $\frac{m}{\Lambda_{QCD}}$.

• After various rescalings this single parameter can be mapped to the parameter T_0 that controls the diverging tachyon in the IR.

• There is also x_f that has become continuous in the large N_c Veneziano limit.

The effective potential

For solutions $T = T_* = constant$ the relevant non-linear action simplifies

$$\mathcal{S} = M^3 N_c^2 \int d^5x \sqrt{g} \left[R - \frac{4}{3} \frac{(\partial\lambda)^2}{\lambda^2} + V_g(\lambda) - x_f V_f(\lambda, T) \right]$$

$$V_f(\lambda, T) = V_0(\lambda)\ e^{-a(\lambda) T_*^2}$$

• Minimizing for T_* we obtain $T_* = 0$ and $T_* = \infty$. The effective potential for λ is

♠ $T_* = 0$, $V_{eff} = V_g(\lambda) - x V_0(\lambda)$ with a IR fixed point at $\lambda = \lambda_*(x_f)$.

♠ $T_* = \infty$, $V_{eff} = V_g(\lambda)$ with no fixed points.

Condensate dimension at the IR fixed point

• By expanding the DBI action we obtain the IR tachyon mass at the IR fixed point $\lambda = \lambda_*$ which gives the chiral condensate dimension:

$$-m_{\rm IR}^2 \ell_{\rm IR}^2 = \Delta_{\rm IR}(4-\Delta_{\rm IR}) = \frac{24a(\lambda_*)}{h(\lambda_*)(V_g(\lambda_*) - x_f V_0(\lambda_*))}$$

• Must reach the Breitenlohner-Freedman (BF) bound (horizontal line) at some x_c.

• x_c marks the *conformal phase transition*

Kaplan+Lee+Son+Stephanov

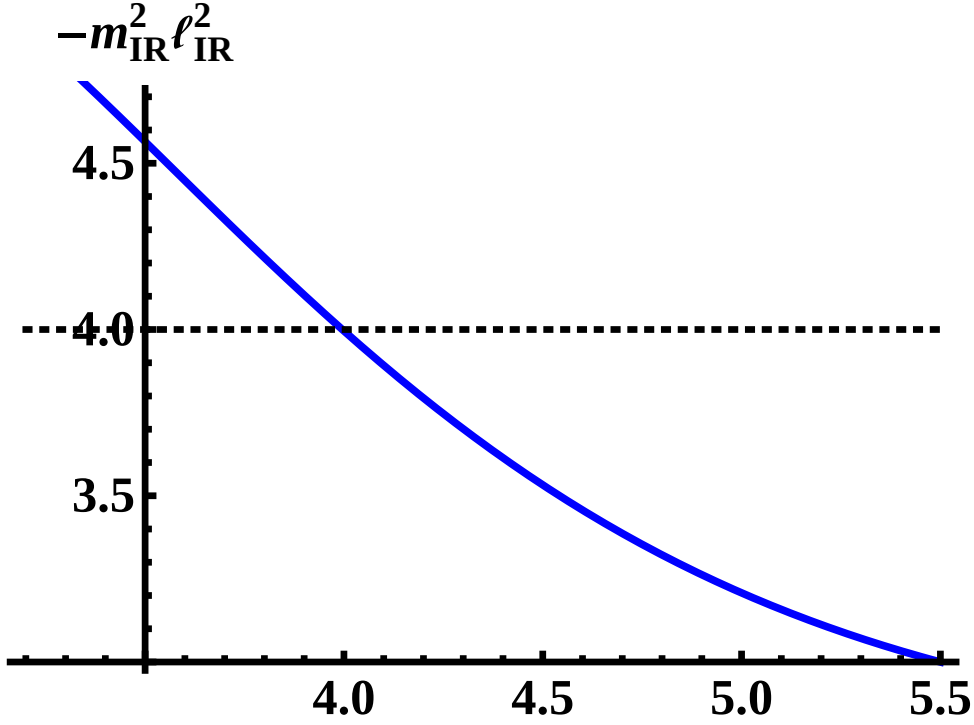

We obtain: $3.7 \lesssim x_c \lesssim 4.2$

UV mass vs IR parameter

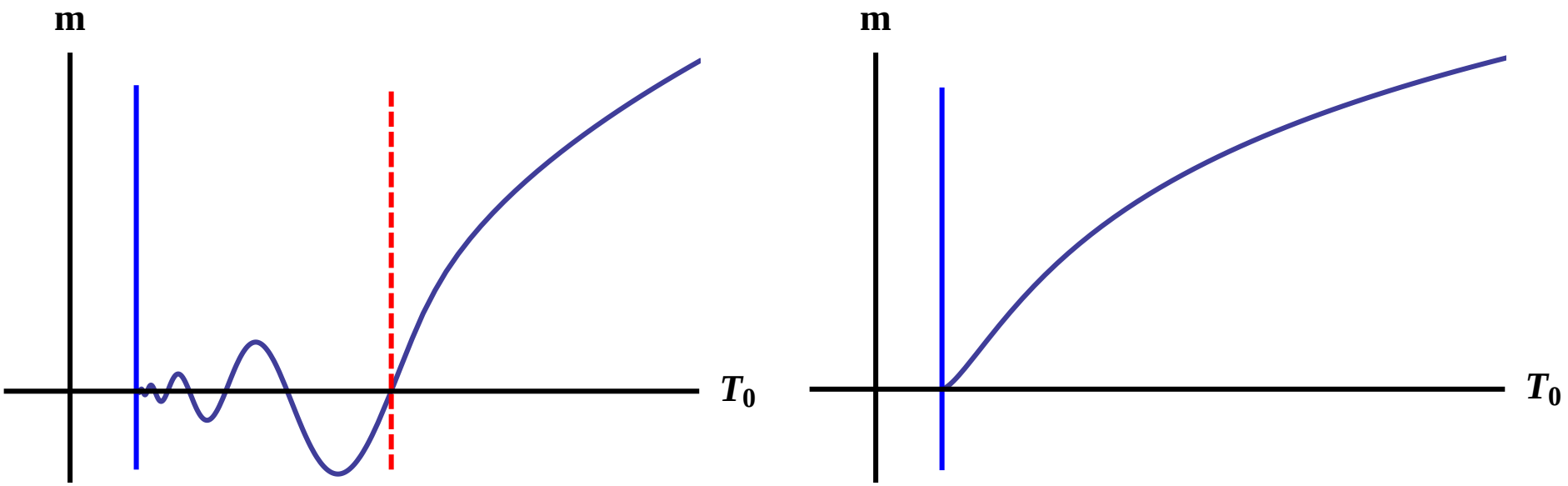

• Left figure: Plot of the UV Mass parameter m, as a function of the IR T_0 scale, for $x < x_c$.

• Right figure: Similar plot for $x \geq x_c$.

• Such plots are sketched from the numerics, analytical expansions and some guesses.

• The tachyon starts at the boundary, evolves into the sinusoidal form for a while, $T \sim r^2 \sin[k \log r + \phi]$, and then at the end diverges. Similar behavior seen at

Kutasov+Lin+Parnachev

• For the n-th solution, the tachyon changes sign n times before diverging in the IR.

• At $m = 0$ there is an ∞ number of saddle point solutions (Efimov-like minima)

• The Efimov minima have free energies ΔE_n with

$$\Delta E_0 > \Delta E_1 > \Delta E_2 > \cdots$$

Efimov spiral

Ongoing work: $\sigma(m)$ dependence

❑ For $x < x_c$ spiral structure

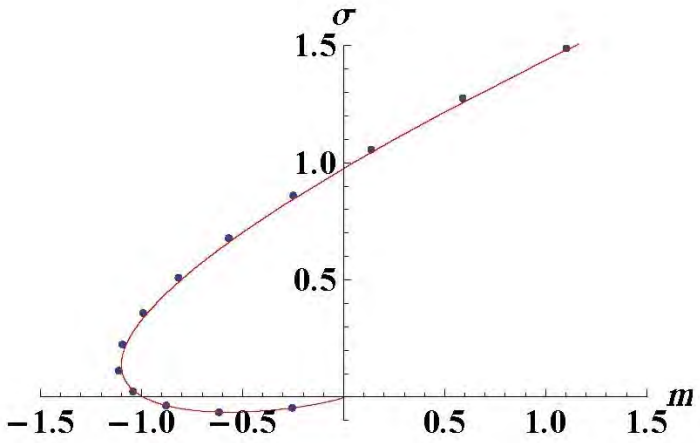

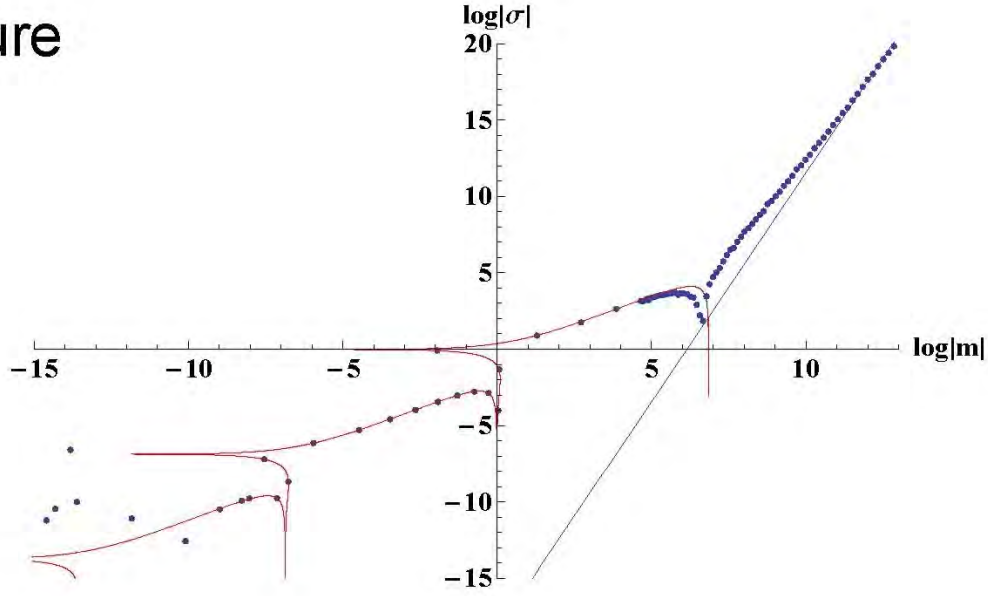

• This suggests that the presence of double trace deformations can alter the ground state of the system and make the second Effimov vacuum be the ground state.

Recap

- For $x = 0$, the theory has a mass gap, and confines.

- $0 < x < x_c \simeq 4$ the theory has chiral symmetry breaking, massless pions, and gapped spectrum otherwise.

- $x_c < x < \frac{11}{2}$ the theory is chirally symmetric, and flows to a non-trivial fixed point in the IR.

Walking

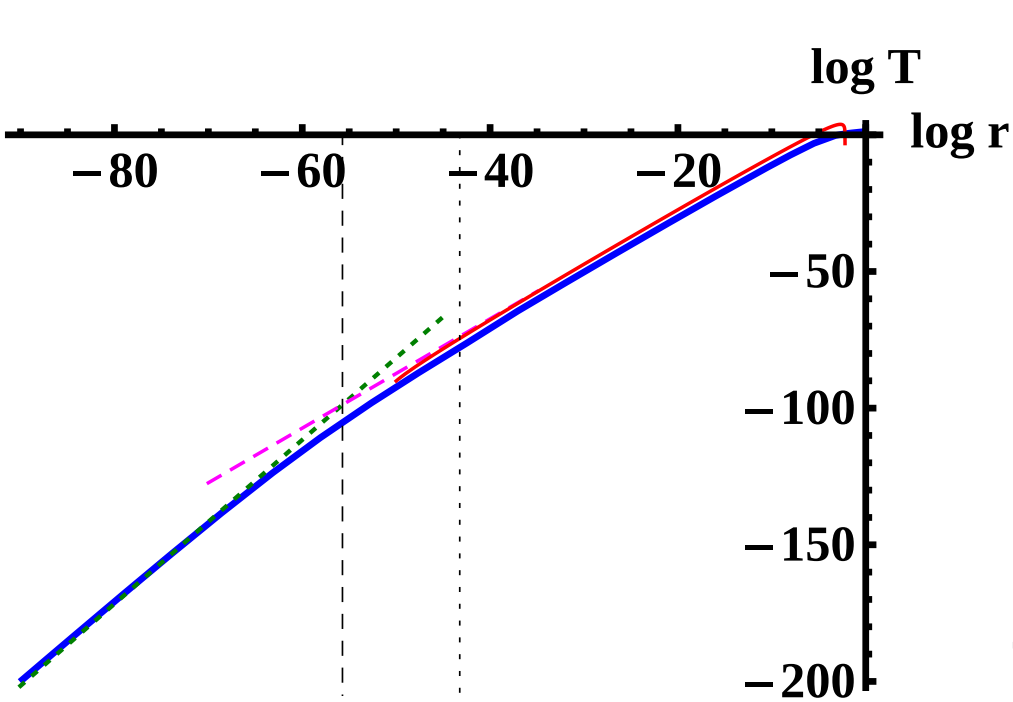

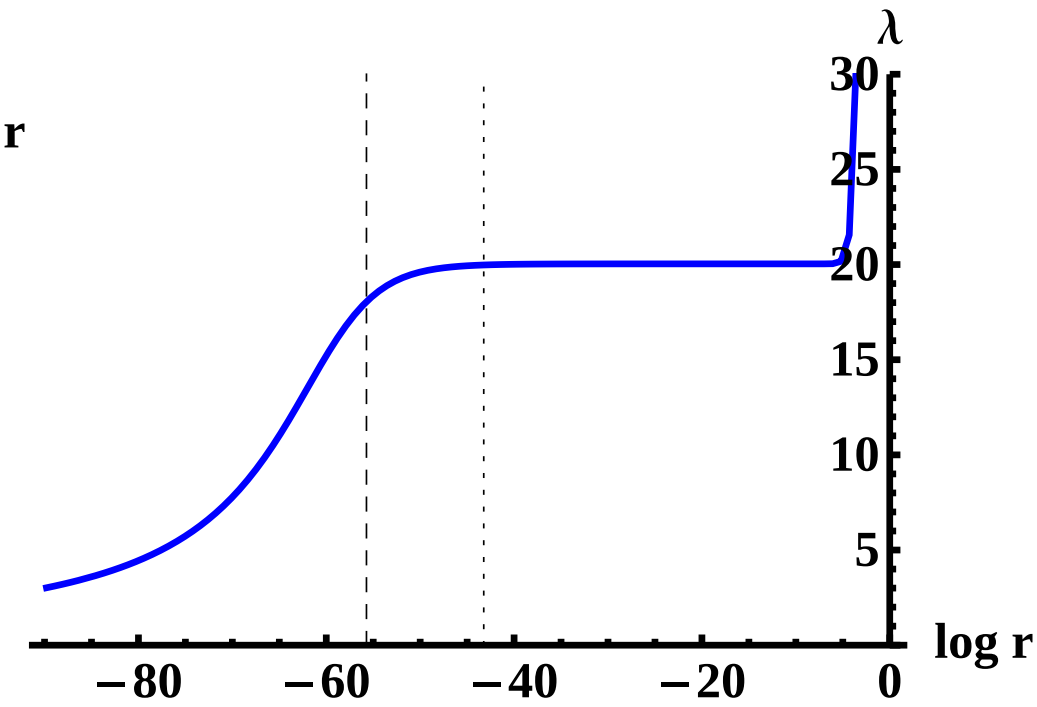

The tachyon $\log T$ (left) and the coupling λ (right) as functions of $\log r$ for an extreme walking background with $x = 3.992$. The thin lines on the left hand plot are the approximations used to derive the BKT scaling.

BKT/Miransky scaling

We obtain BKT-Miransky scaling:

$$\sigma \sim \Lambda_{\rm UV}^3 \ \exp\left(-\frac{2K}{\sqrt{\lambda_* - \lambda_c}}\right) \sim \Lambda_{\rm UV}^3 \ \exp\left(-\frac{2\hat{K}}{\sqrt{x_c - x}}\right) \ .$$

and the function that controls $K, \hat{K}$ is

$$\Delta_{\rm IR}(4-\Delta_{\rm IR}) = -m_{\rm IR}^2 \ell_{\rm IR}^2 = G(\lambda_*, x) \equiv \left.\frac{24a(\lambda)}{h(\lambda)(V_g(\lambda) - xV_{f0}(\lambda))}\right|_{\lambda=\lambda_*} ,$$

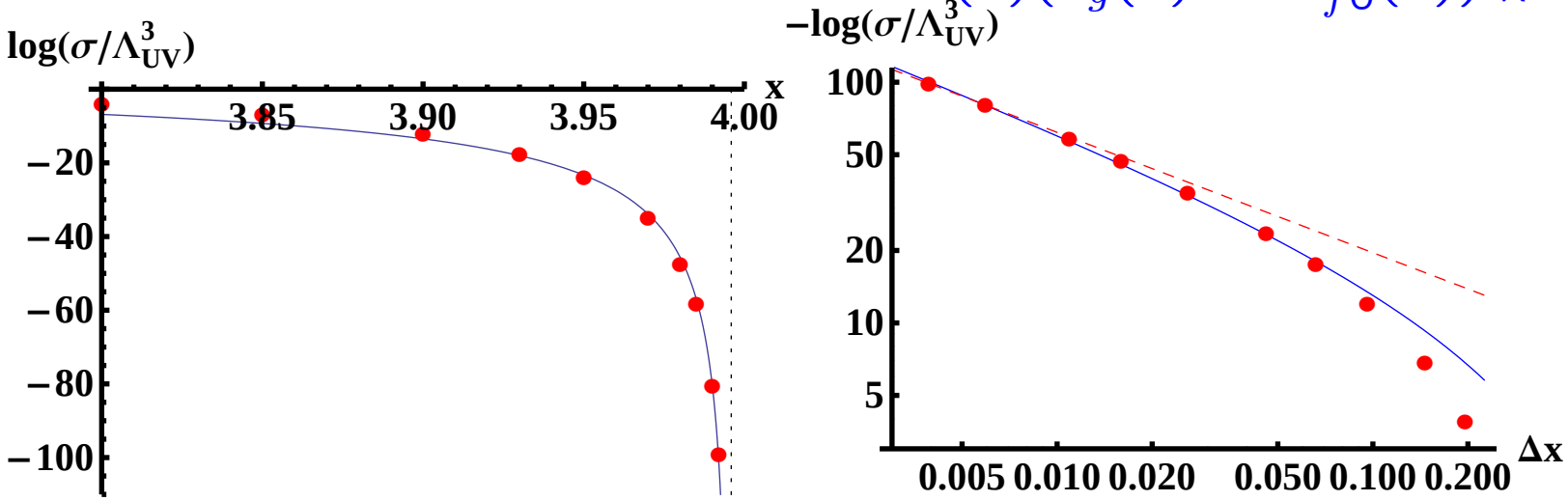

Left: $\log(\sigma/\Lambda^3)$ as a function of x (dots), compared to a BKT scaling fit (solid line). The vertical dotted line lies at $x = x_c$. Right: the same curve on log-log scale, using $\Delta x = x_c - x$.

Spectra

• The main difference from all previous calculations is that here flavor back reacts on color.

• In the singlet sector the glueballs and mesons mix to leading order and the spectral problem becomes complicated.

• The preliminary conclusions are:

♠ All masses follow Miransky scaling in the walking region.

♠ There is no dilaton

♠ There are several level crossings as x_f varies but they seem accidental

♠ The situation with the S-parameter is still unclear.

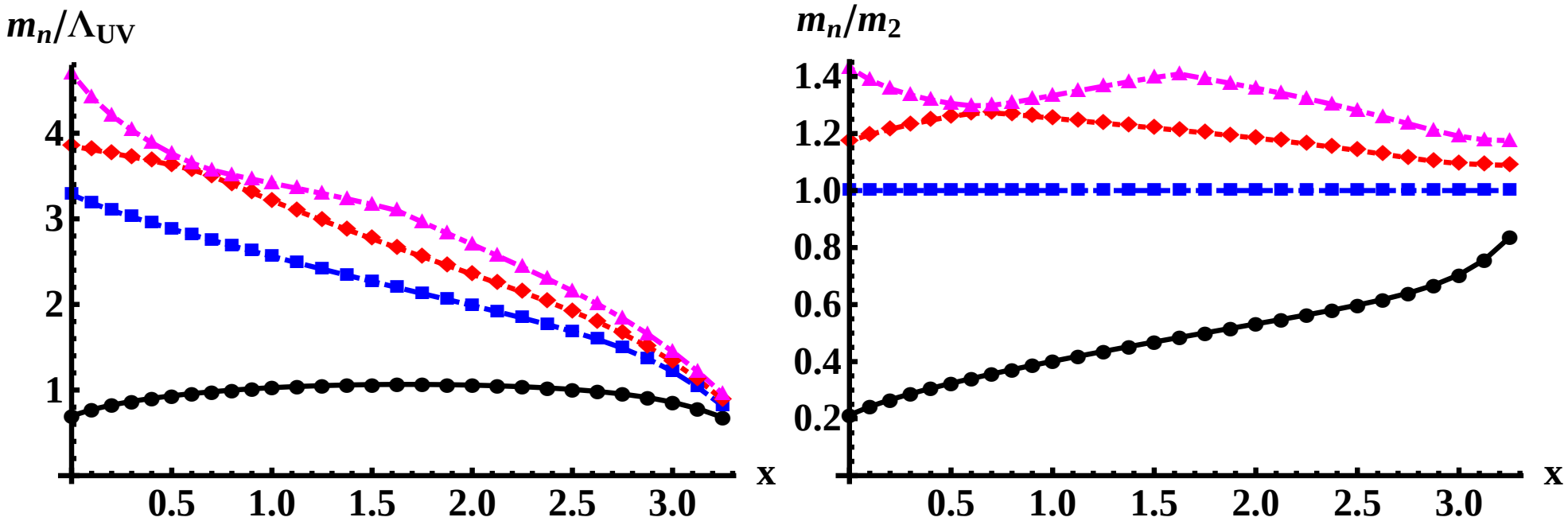

The masses of the first four modes of the scalar mesons of the $U(1)$ sector for potentials I. Left: the masses in the units of Λ_{UV} as a function of x. Right: the ratios m_n/m_2 of the masses of the modes. We chose to normalize to the second mode since that makes the x-dependence of the ratios better visible.

Finite Temperature

Alho+Jarvinnen+Kajantie+E.K.+Tuominnen

Choices:

- Potentials I vs II
- Value of $0 < W_0 < \frac{24}{11}$
- Fixed point exists for all x, or not

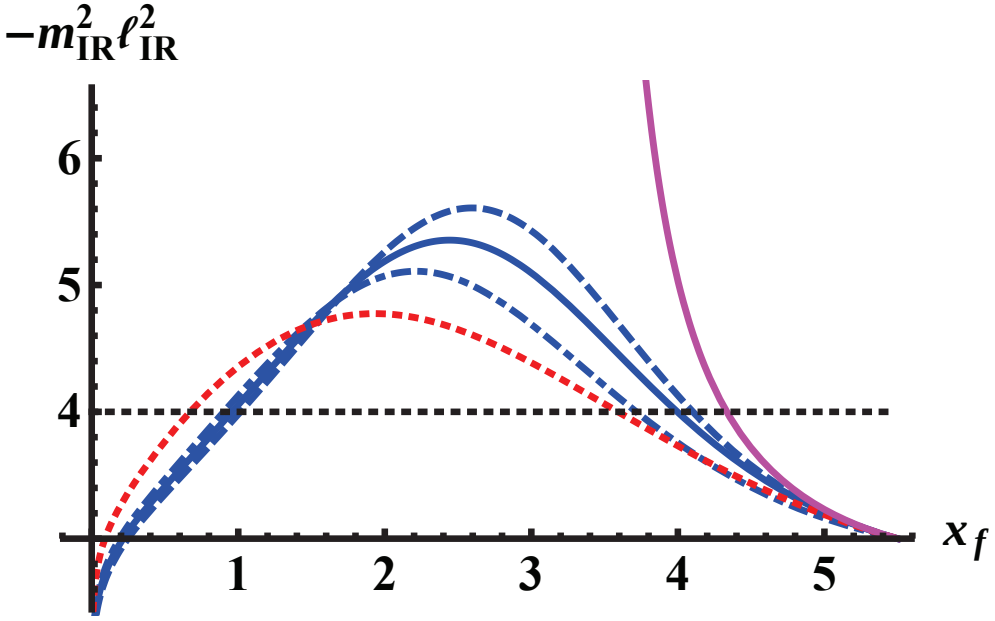

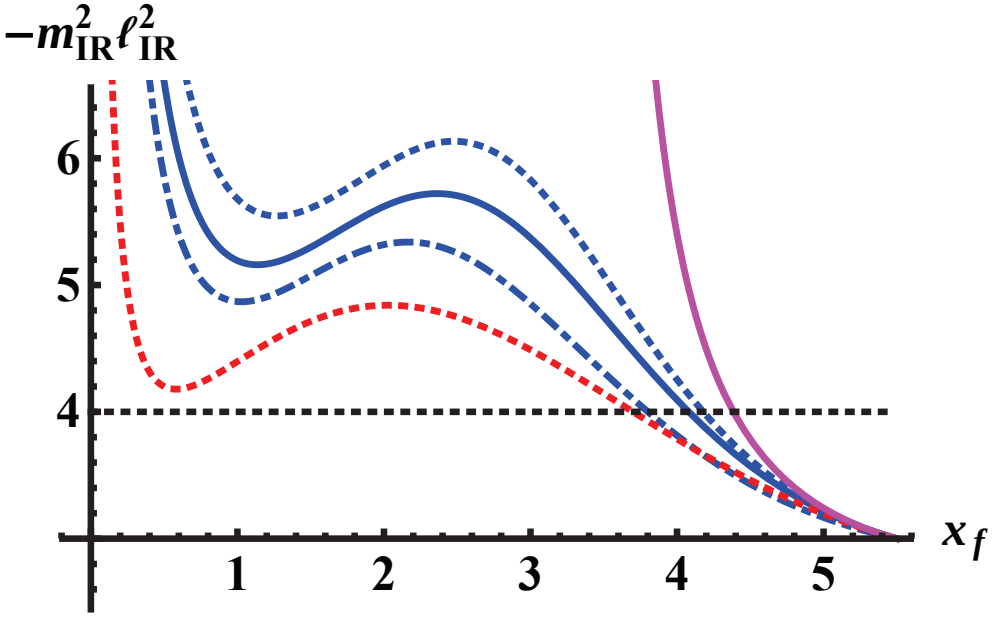

Finite Temperature: the generic phase diagram

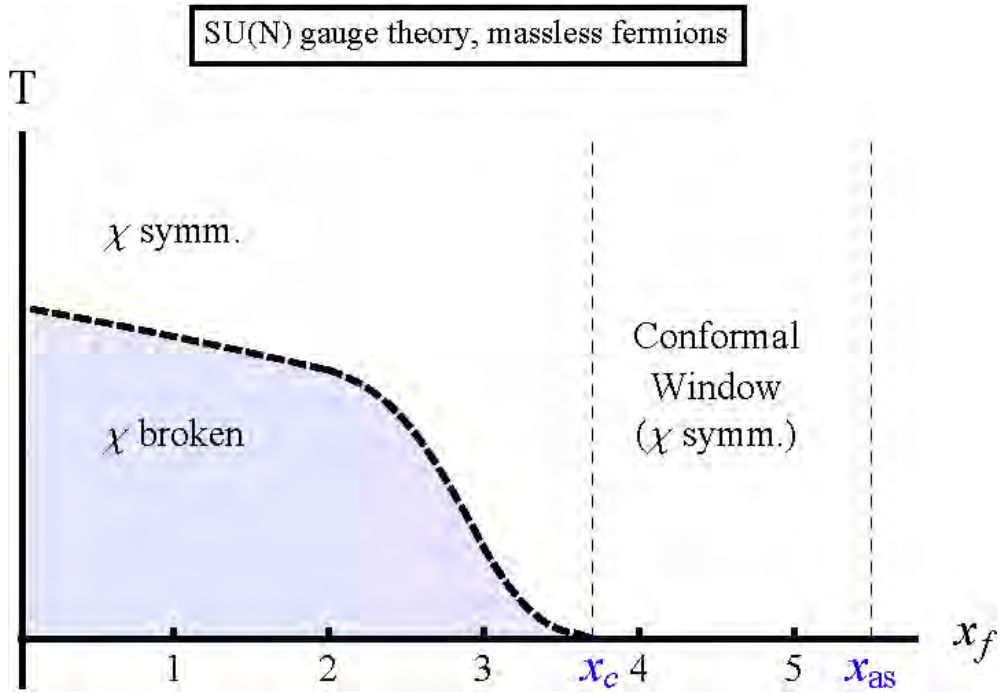

Qualitative behavior of the transition temperature between the low and high T phases of V-QCD matter.

The different types of blackholes

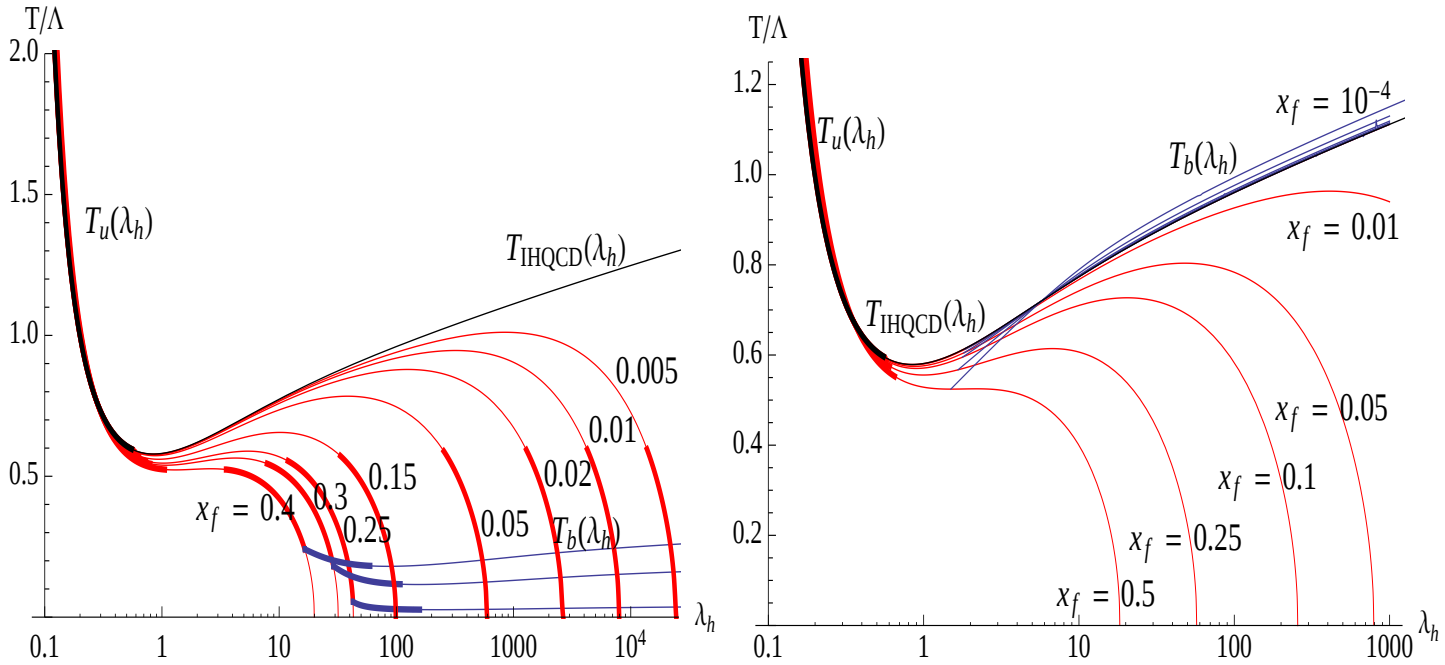

Figure 22: $T(\lambda_h)$ for various small values of x_f and for potential I, $W_0 = 24/11$ (*Left*) or for potential II, $W_0 = 12/11$ (*Right*). The black curve is the IHQCD limit. The chirally symmetric $T_u(\lambda_h) \equiv T(\lambda_h, \tau = 0)$ branch asymptotes to the IHQCD curve as $x_f \to 0$, for both potentials. The chirally broken $T_b(\lambda_h) \equiv T(\lambda_h, \tau_h(\lambda_h, m_q = 0))$ branches behave very differently for PotI and PotII. For PotI T_b is absent at such low x_f and all phases are chirally symmetric (see also Fig. 18). For PotII the curves T_b follow very closely T_s and, correspondingly, $T_h \approx T_s$ (see Fig. 15).

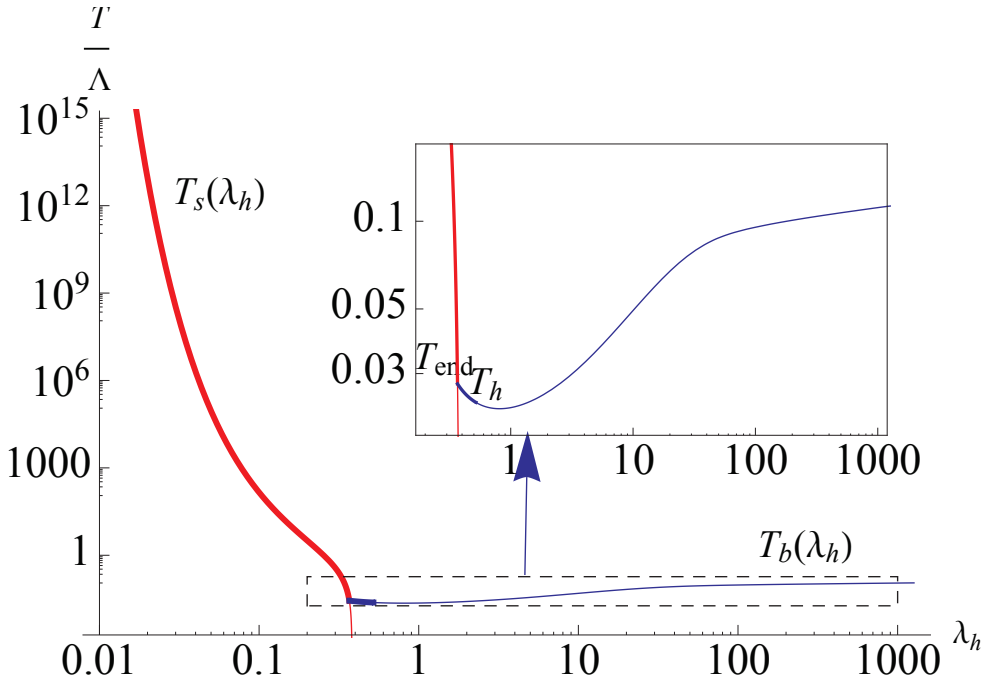

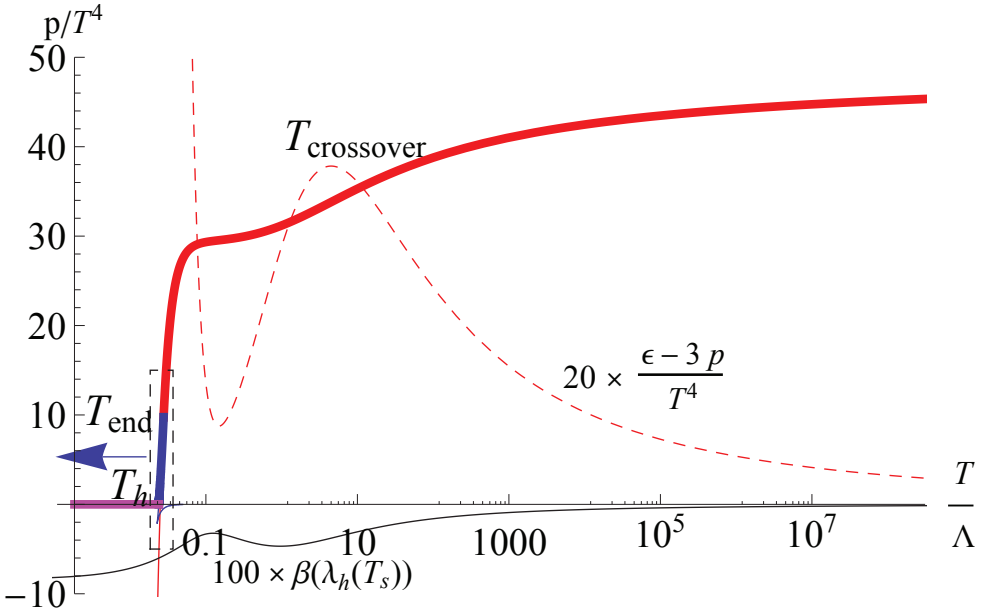

Examples of the $T_{\rm end}$, T_h and $T_{\rm crossover}$ transitions in potential II with Stefan-Boltzmann -normalization of $\mathcal{L}_{\rm UV}$ and with $x_f = 3$ The curving of $T_s(\lambda_h)$ at $\lambda_h \sim 0.2$, $T \sim 2$ is related to the crossover transition. *Right*: an overview of the pressure in the same case, also showing the interaction measure, the peak of which determines the position of $T_{\rm crossover}$. The black curve shows the vacuum beta function, scaled to fit, as a function of temperature in the symmetric phase, so that $\beta(T) = \beta(\lambda_s(T))$, where $\lambda_s(T)$ is the inverse function of $T_s(\lambda_h)$. The walking maximum of the beta function clearly coincides with the plateau related to $T_{\rm Crossover}$, confirming that the $p/T^4 \sim$ constant phase below $T_{\rm Crossover}$ is indeed the quasi-conformal phase related to walking dynamics.

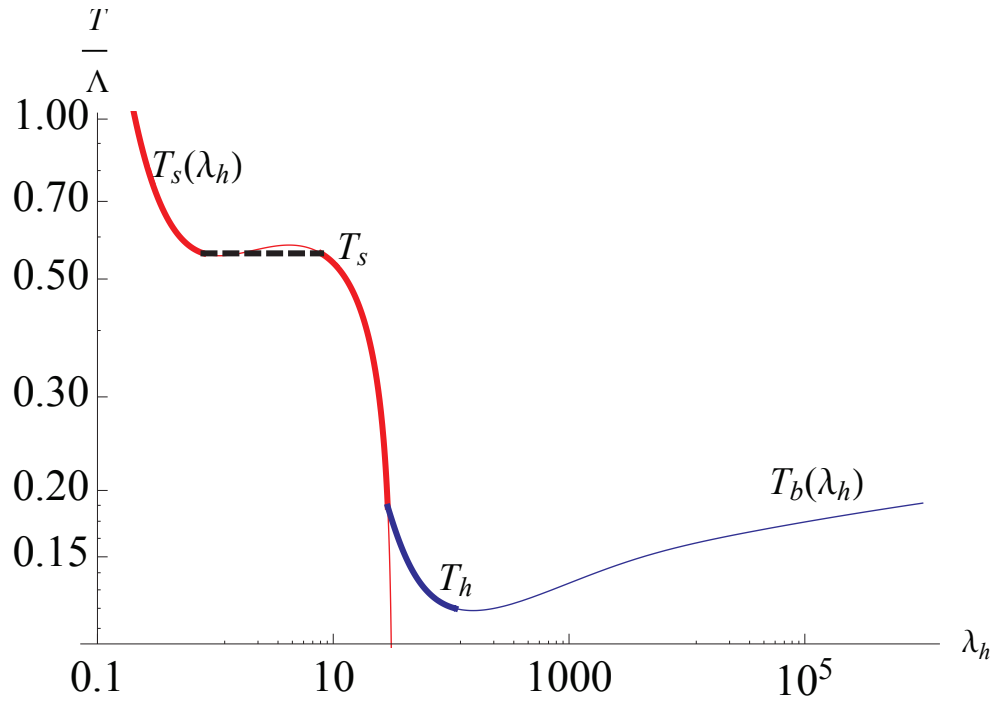

An example of the T_S transition in potential I with $W_0 = 24/11$ and with $x_f = 0.3$ The local maximum and minimum which generate the 1st order T_S -transition.

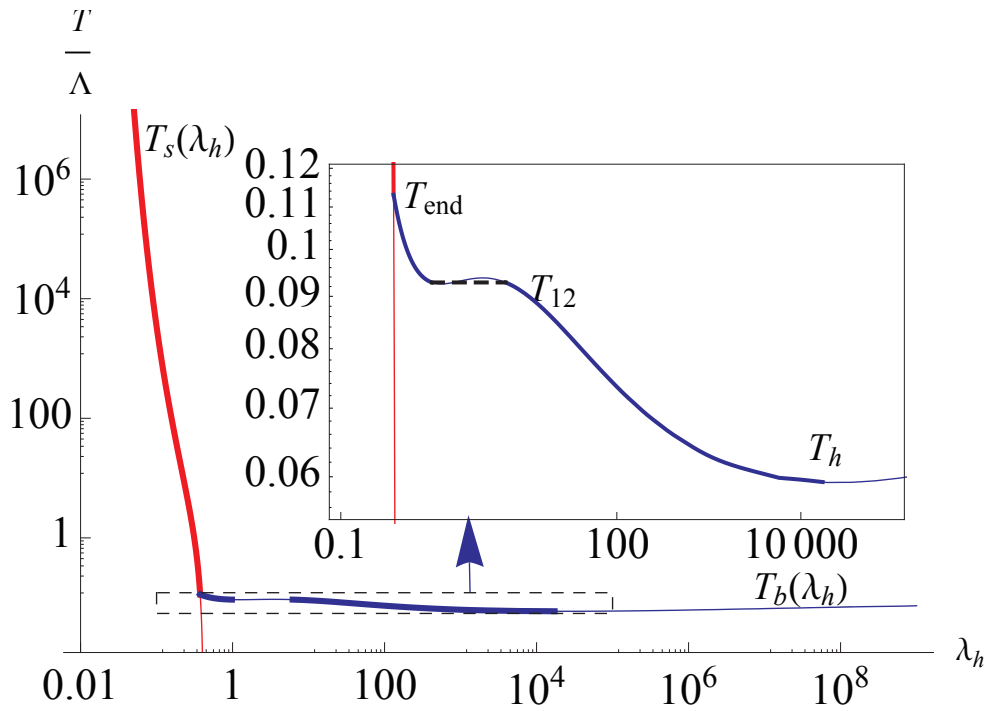

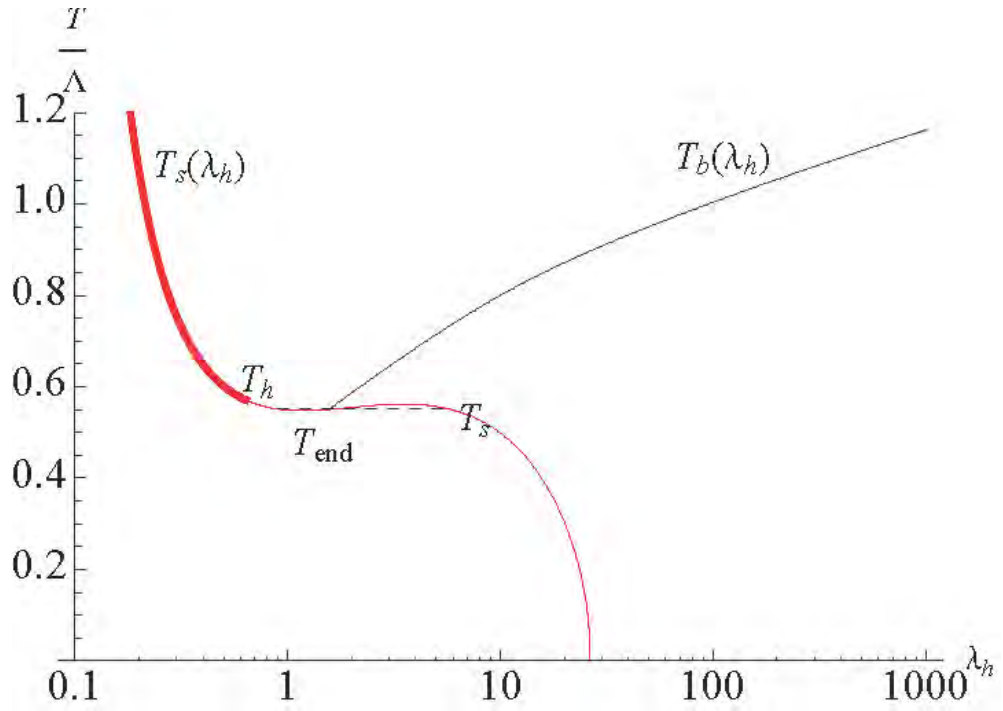

Left: An example of the T_{12} transition in potential I with $W_0 = 12/11$ and with $x_f = 3.5$. The overall structure of $T(\lambda_h)$, with an inset showing the maximum and minimum in more detail.

Right: An example of a configuration where all but the crossover and hadronisation transitions $T_{\rm crossover}$, T_h, are in the thermodynamically unstable region, in the initial stages of the approach to the IHQCD limit. The potential is II with $W_0 = 12/11$ and with $x_f = 0.4$ Note that everything to the right of the T_h transition is in the unstable phase.

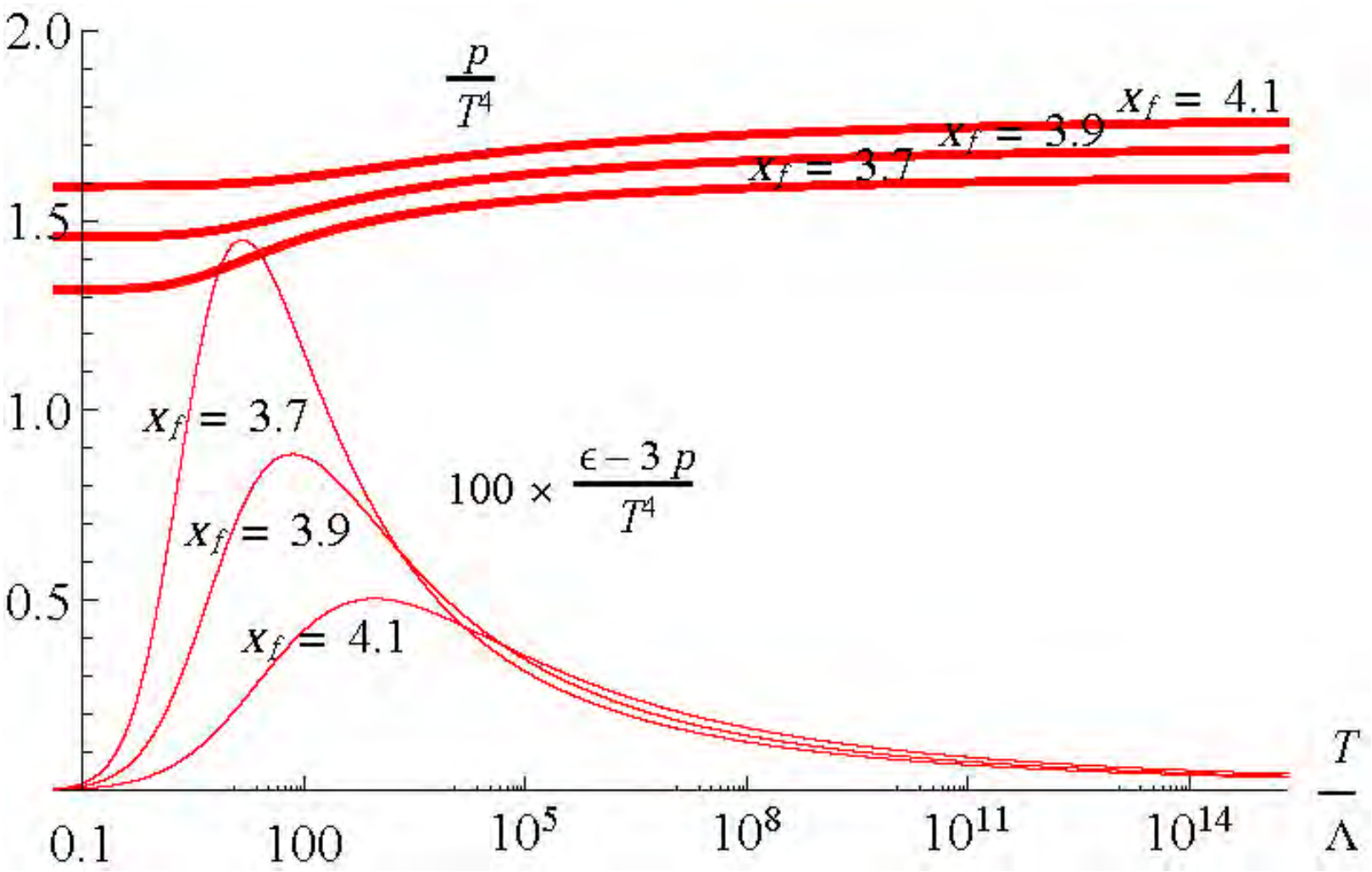

Thermodynamics for some values of x_f within the conformal window, computed for PotI. Note that in the conformal window always $\tau = 0$ and the functions $a(l)$, $\Phi(l)$ do not affect the result.

Finite small mass

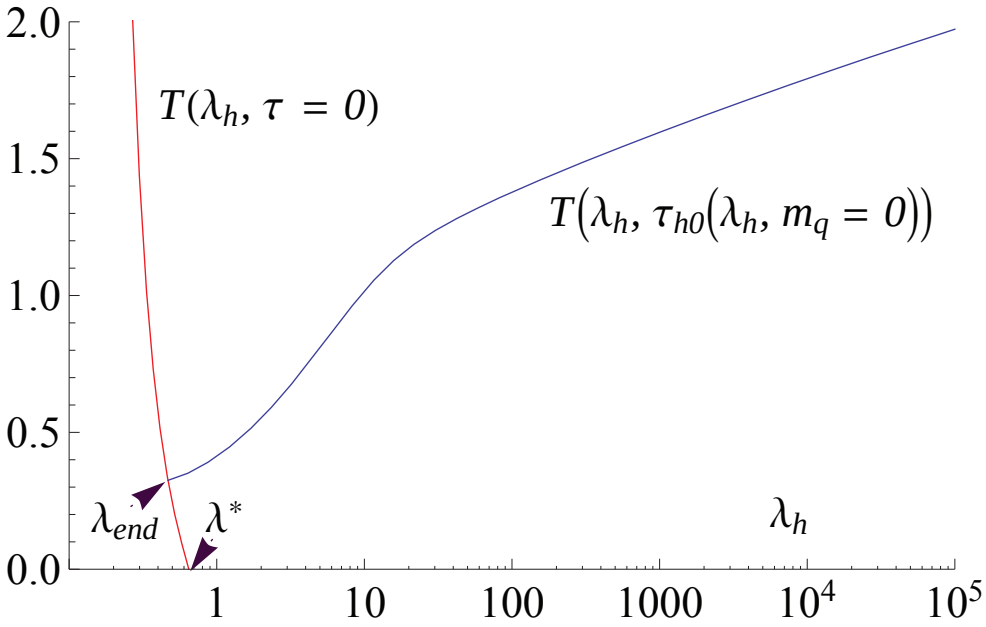

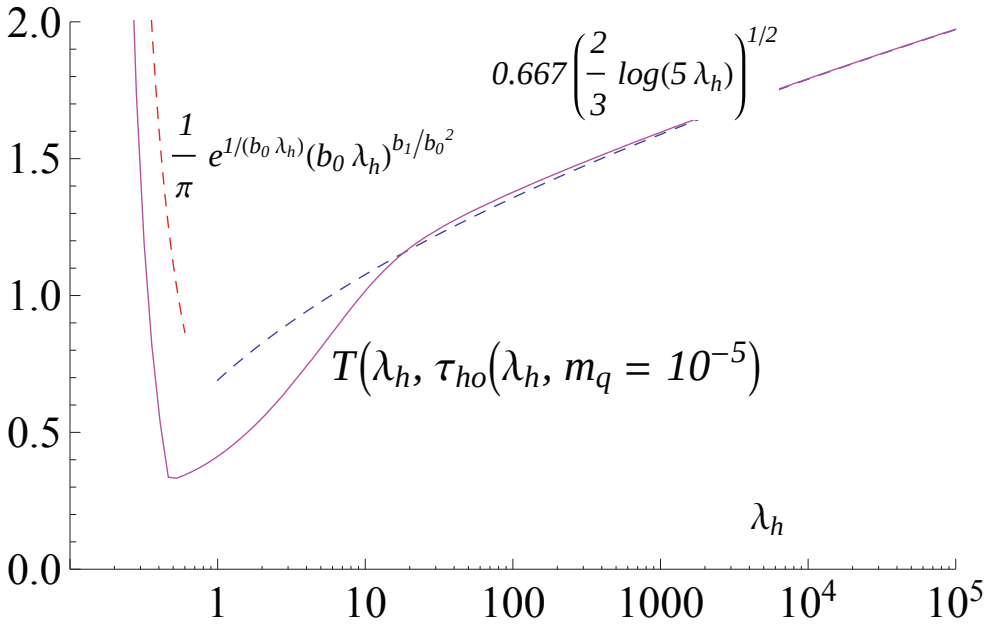

The phase diagrams

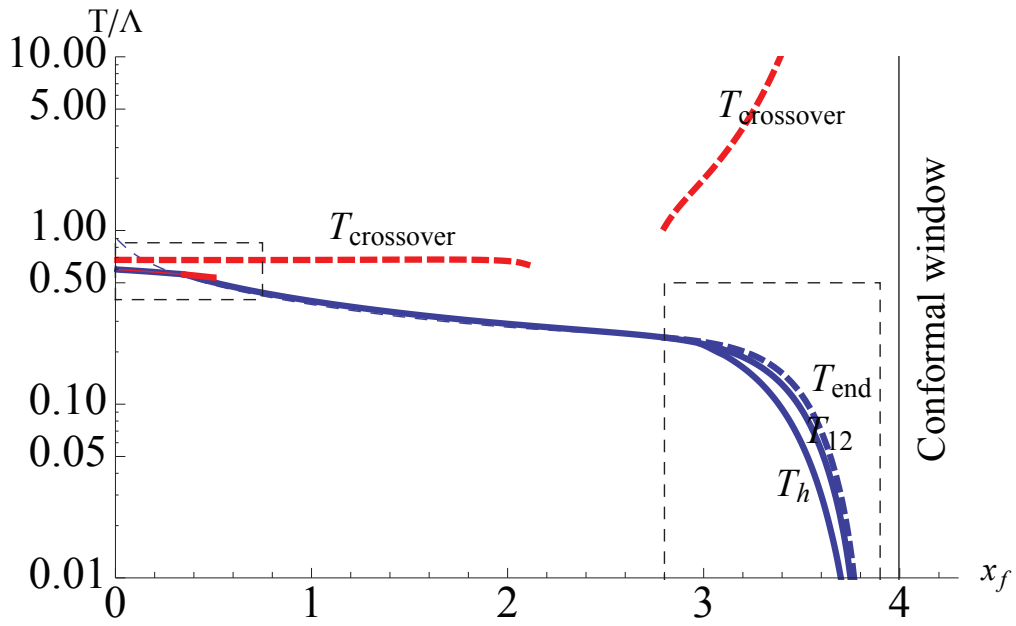

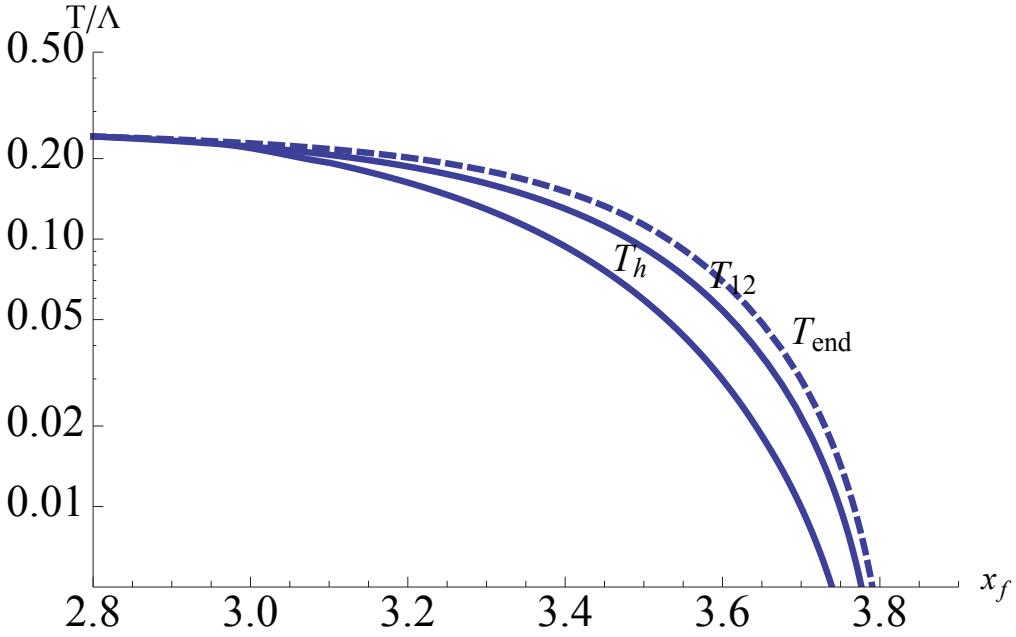

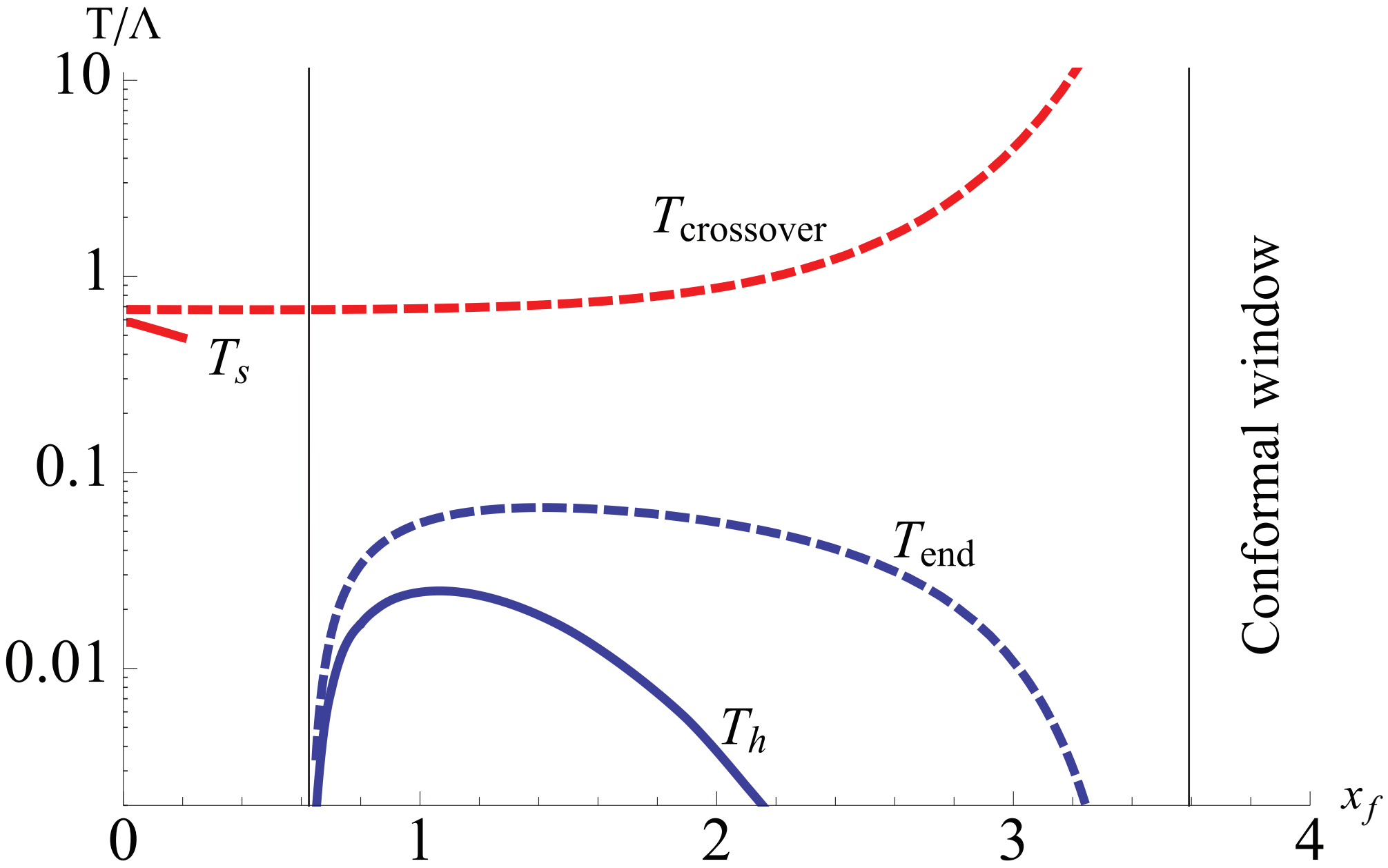
T/Λ
10
1
0.1
0.01
$T_{\rm crossover}$
T_s
$T_{\rm end}$
T_h
Conformal window
0
1
2
3
4
x_f

Outlook

There are many directions that need to be explored:

- Further analysis of the meson spectra at $T = 0$ and their asymptotics at high energy.

- Settle the question of the S parameter for technicolor applications.

- Study energy loss of quarks in QGP (with full backreaction).

- Study the phase diagram at finite density and applications to CMT.

- Transport and hydrodynamics in the walking region.

- Addition of multi-trace operators of the quark mass operators. These affect the walking region, rearrange the Efimov vacua, and are generated in technicolor setups.

- "Model building": Construction of realistic technicolor models.

.

Thank you

This research has been co-financed by the European Union (European Social Fund, ESF) and Greek national funds through the Operational Program "Education and Lifelong Learning" of the National Strategic Reference Framework (NSRF), under the grants schemes "Funding of proposals that have received a positive evaluation in the 3rd and 4th Call of ERC Grant Schemes" and the program "Thales"

N=1 sQCD

The case of $\mathcal{N} = 1$ $SU(N_c)$ superQCD with N_f quark multiplets is known and provides an interesting (although much more complex) example for the non-supersymmetric case.

Seiberg

• $x = 0$ the theory has confinement, a mass gap and N_c distinct vacua associated with a spontaneous breaking of the leftover R symmetry Z_{N_c}.

• At $0 < x < 1$, the theory has a runaway ground state.

• At $x = 1$, the theory has a quantum moduli space with no singularity. This reflects confinement with χSB.

• At $x = 1 + \frac{1}{N_c}$, the moduli space is classical (and singular). The theory confines, but there is no χSB.

- At $1+\frac{2}{N_c} < x < \frac{3}{2}$ the theory is in the non-abelian magnetic IR-free phase, with the magnetic gauge group $SU(N_f - N_c)$ IR free.

- At $\frac{3}{2} < x < 3$, the theory flows to a CFT in the IR. (conformal window)

Near $x = 3$ this is the Banks-Zaks region where the original theory has an IR fixed point at weak coupling. Moving to lower values, the coupling of the IR $SU(N_c)$ gauge theory grows.

However near $x = \frac{3}{2}$ the dual magnetic $SU(N_f - N_c)$ is in its Banks-Zaks region, and provides a weakly coupled description of the IR fixed point theory.

- At $x > 3$, the theory is IR free.

Walking region+Technicolor

• Technicolor: EW symmetry breaking is due to a new strong gauge interaction with $\Lambda_{TC} \sim 1 TeV$.

• The EW Higgs is scalar TC meson and the vev is due to a condensate of TC fermions $\langle H \rangle \sim \langle \bar{\psi}_{TC} \psi_{TC} \rangle$ from TC chiral symmetry breaking.

• The Higgs vev is the TC f_π and should be ~ 250 GeV.

• The composite Higgs couplings to the SM fermions χ are now four-fermi terms,

$$H \bar{\chi} \chi \sim \bar{\psi}_{TC} \psi_{TC} \; \bar{\chi} \chi$$

and should be generated by a new (ETC) interaction at a higher scale, Λ_{ETC}.

• There are some important problems with this idea:

♠ At the qualitative level: it relies on non-perturbative physics and therefore is not easily controlable/calculable.

♠ There can be important flavor changing processes (that are suppressed in the SM)

♠ To get the correct size for all masses, the dimension of operators $\psi_{TC}\psi_{TC}$ must be close to two (instead of 3 in perturbation theory).

♠ The dimensionless quantity

Peskin+Takeuchi

$$S = \frac{d}{dq^2}(\Pi_V(q^2) - \Pi_A(q^2))\Big|_{q^2=0} \quad , \quad \left(\delta_{\mu\nu} - \frac{q_\mu q_\nu}{q^2}\right)\Pi_i(q^2) \equiv \langle J^i_\mu(q) J^i_\nu(0)\rangle$$

is $\mathcal{O}(1)$ in generic theories from the spectral decomposition+sum rules, but EW data imply that its should be $\mathcal{O}(10^{-2})$.

♠ It has been argued by many scientists that a way out of the above is a TC theory that is near conformal ("walking") in the TC regime,

Holdom

♠ This theory is expected to have a light scalar, "the dilaton", namely the singlet scalar meson (σ-meson), that is important for making the S parameter small.

Yamawaki

♠ Despite a lot of work in the last 15 years, whether such a theory exists, and whether it has the required properties has remained elusive till now, because lattice techniques are hard to apply.

♠ It has been argued recently that strongly coupled ty models based on the hard-wall or soft wall holographic models have $S \sim \mathcal{O}(1)$

Rubakov+Levkov+Troitsky+Zenkevich

Below the BF bound

- Correlation of the violation of BF bound and the conformal phase transition

- For $\Delta_{\rm IR}(4-\Delta_{\rm IR})<4$

$$T(r)\sim m_q r^{4-\Delta_{\rm IR}}+\sigma r^{\Delta_{\rm IR}}$$

- For $\Delta_{\rm IR}(4-\Delta_{\rm IR})>4$

$$T(r)\sim C r^2 \sin\left[(\mathrm{Im}\Delta_{\rm IR})\log r+\phi\right]$$

Two possibilities:

- $x>x_c$: BF bound satisfied at the fixed point $\Rightarrow$ only trivial massless solution ($T\equiv 0$, ChS intact, fixed point hit)

- $x<x_c$: BF bound violated at the fixed point $\Rightarrow$ a nontrivial massless solution exists, which drives the system away from the fixed point.

Conclusion: *phase transition* at $x=x_c$

Matching to QCD

- $V_g(\lambda)$ is fixed from glue.

- The UV is adjusted to perturbative QCD.

$$V_g \sim V_0 + \mathcal{O}(\lambda) \quad , \quad V_0 \sim W_0 + \mathcal{O}(\lambda)$$

$$V_0 - xW_0 = \frac{12}{\ell_{UV}^2}$$

- W_0 is one of the most important parameters of the models.

• There are two classes of tachyon potentials:

♠ Type I: $T \sim e^{Cr}$ as $r \to \infty$.

♠ Type II $T \sim \sqrt{r}$ as $r \to \infty$.

• In all cases the "regular" IR solution depends on a single undetermined constant (instead on two).

• The phase structure is essentially independent of IR choices.

Varying the model

"prediction" for x_c

After fixing UV coefficients from QCD, there is still freedom in choosing the leading coefficient of V_0 at $\lambda \to 0$ and the IR asymptotics of the potentials

Thick blue $\to V_I$

Thin red $\to V_{II}$

Resulting variation of the edge of conformal window

$$3.7 \lesssim x_c \lesssim 4.2$$

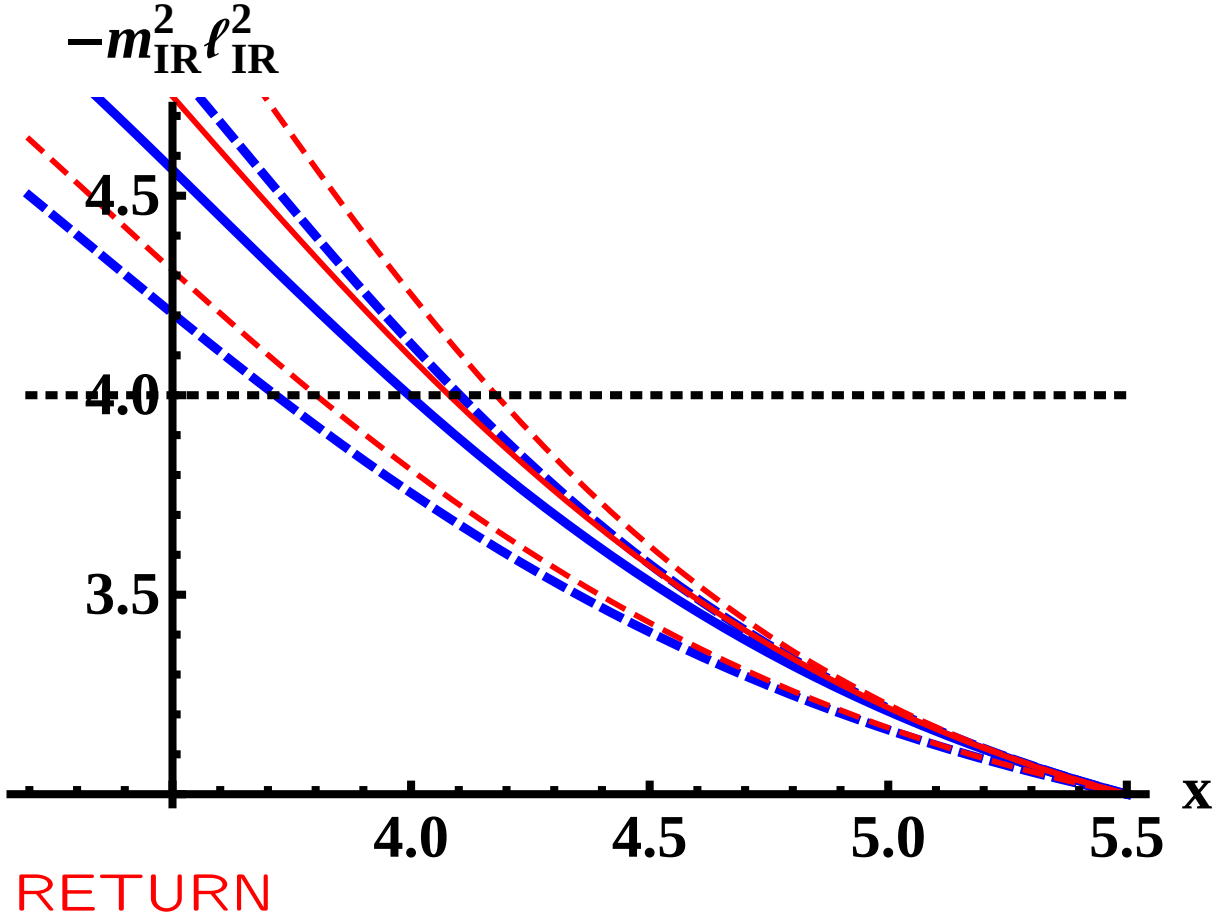

RETURN

The IR fixed point

$$V_{\rm eff}(\lambda) = V_g(\lambda) - xV_0(\lambda)$$

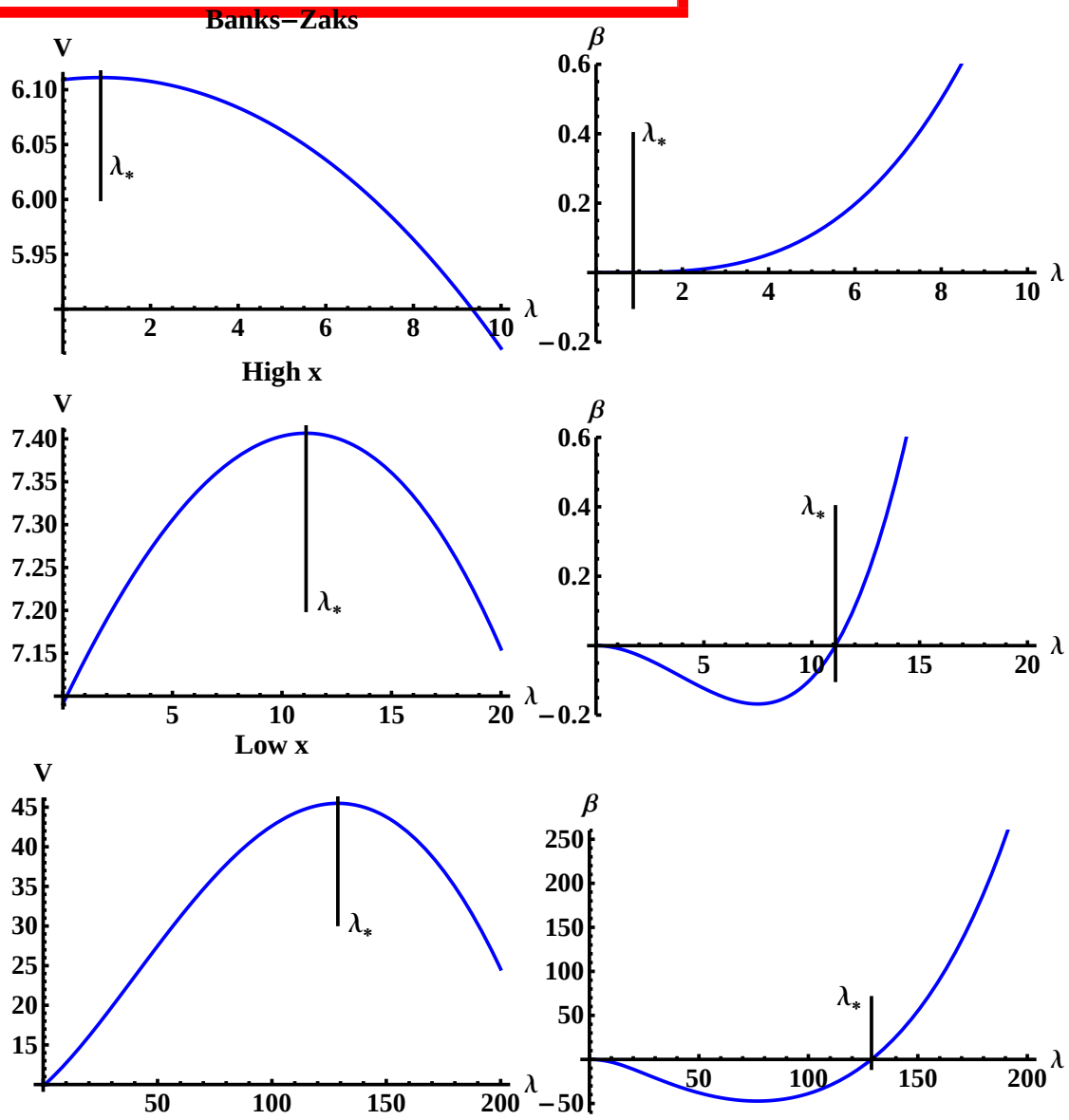

Two possibilities: (a) The maximum exists for all x. (b) The maximum exists for $x > x_*$.

Matching to QCD: UV

- As $\lambda \to 0$ we can match:

♠ $V_g(\lambda)$ with (two-loop) Yang-Mills β-function.

♠ $V_g(\lambda) - xV_0(\lambda)$ with QCD β-function.

♠ $a(\lambda)/h(\lambda)$ with anomalous dimension of the quark mass/chiral condensate

- The matching allows to mark the BZ point, that we normalize at $x = \frac{11}{2}$.

- After the matching above we are left with a single undetermined parameter in the UV:

$$V_g \sim V_0 + \mathcal{O}(\lambda) \quad , \quad V_0 \sim W_0 + \mathcal{O}(\lambda)$$

$$V_0 - xW_0 = \frac{12}{\ell_{UV}^2}$$

Matching to QCD: IR

• In the IR, the tachyon has to diverge $\Rightarrow$ the tachyon action $\propto e^{-T^2}$ becomes small

♠ $V_g(\lambda) \simeq \lambda^{\frac{4}{3}}\sqrt{\lambda}$ chosen as for Yang-Mills, so that a "good" IR singularity exists etc.

♠ $V_0(\lambda)$, $a(\lambda)$, and $h(\lambda)$ chosen to produce tachyon divergence: there are several possibilities.

♠ The phase structure is essentially independent of IR choices.

Choice I, for which in the IR

$$T(r) \sim T_0 \exp\left[\frac{81\ 3^{5/6}(115-16x)^{4/3}(11-x)}{812944\ 2^{1/6}}\frac{r}{R}\right] \quad , \quad r \to \infty$$

R is the IR scale of the solution. T_0 is the control parameter of the UV mass.

Choice II: for which in the IR

$$T(r) \sim \frac{27\ 2^{3/4}3^{1/4}}{\sqrt{4619}}\sqrt{\frac{r-r_1}{R}} \quad , \quad r \to \infty$$

R is the IR scale of the solution. r_1 is the control parameter of the UV mass.

The free energy

The free energy difference between the ChS and ChSB $m_q = 0$ solutions

Chiral symmetry breaking solution favored whenever it exists ($x < x_c$)

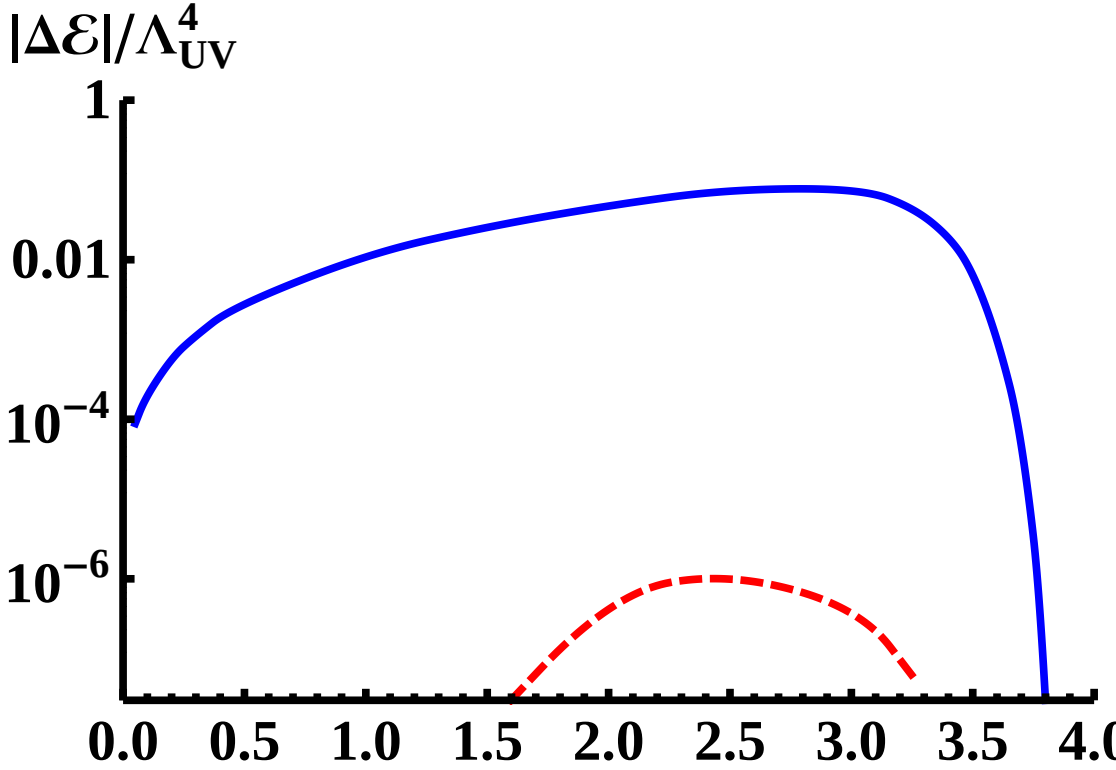

- The Efimov minima have free energies ΔE_n with

$$\Delta E_0 > \Delta E_1 > \Delta E_2 > \cdots$$

Walking

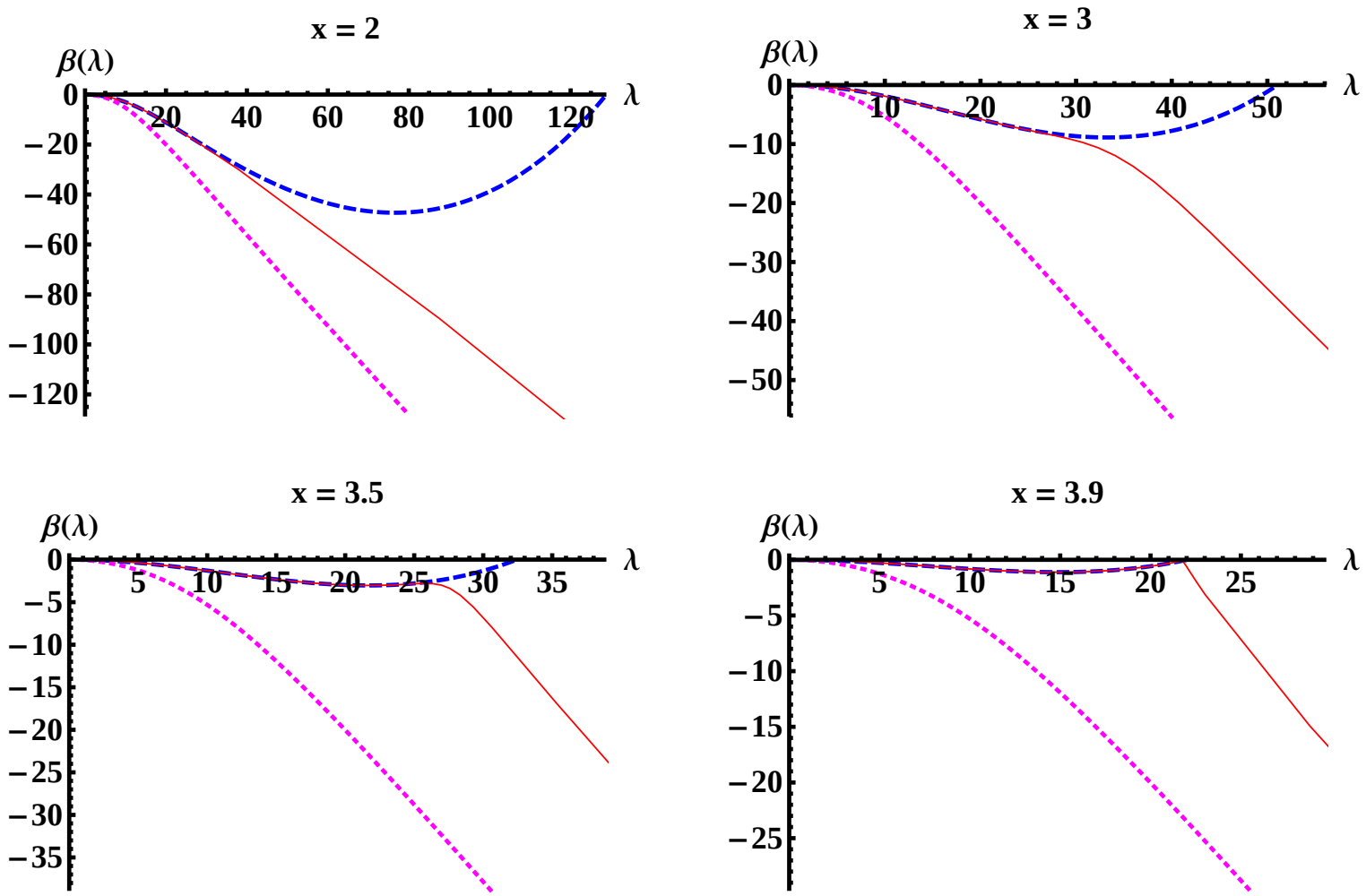

The β-functions for vanishing quark mass for various values of x. The red solid, blue dashed, and magenta dotted curves are the β-functions corresponding to the full numerical solution $(d\lambda/dA)$ along the RG flow, the potential $V_{\text{eff}} = V_g - xV_{f0}$, and the potential V_g, respectively.

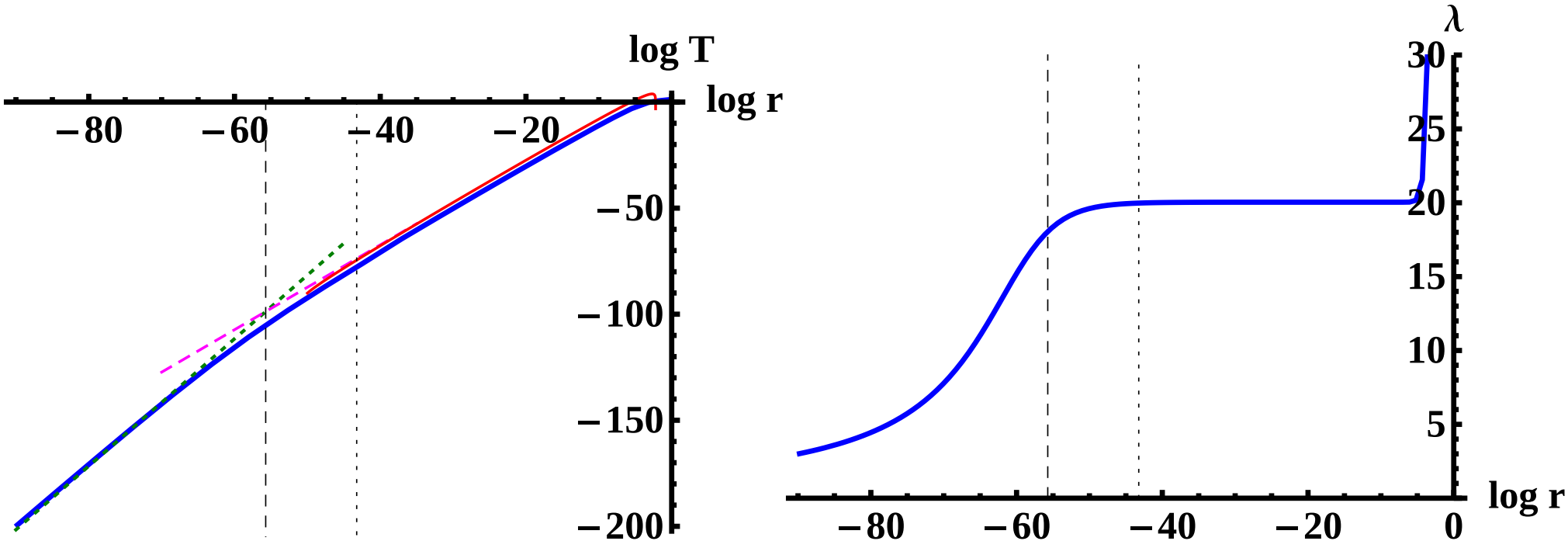

The tachyon $\log T$ (left) and the coupling λ (right) as functions of $\log r$ for an extreme walking background with $x = 3.992$. The thin lines on the left hand plot are the approximations used to derive the BKT scaling.

Holographic β-functions

The second order equations for the system of two scalars plus metric can be written as first order equations for the β-functions

Gursoy+Kiritsis+Nitti

$$\frac{d\lambda}{dA} = \beta(\lambda, T) \quad , \quad \frac{dT}{dA} = \gamma(\lambda, T)$$

The equations of motion boil down to two partial non-linear differential equations for β, γ.

Such equations have also branches as for DBI and non-linear scalar actions the relation of $e^{-A}A'$ with the potentials is a polynomial equation of degree higher than two.

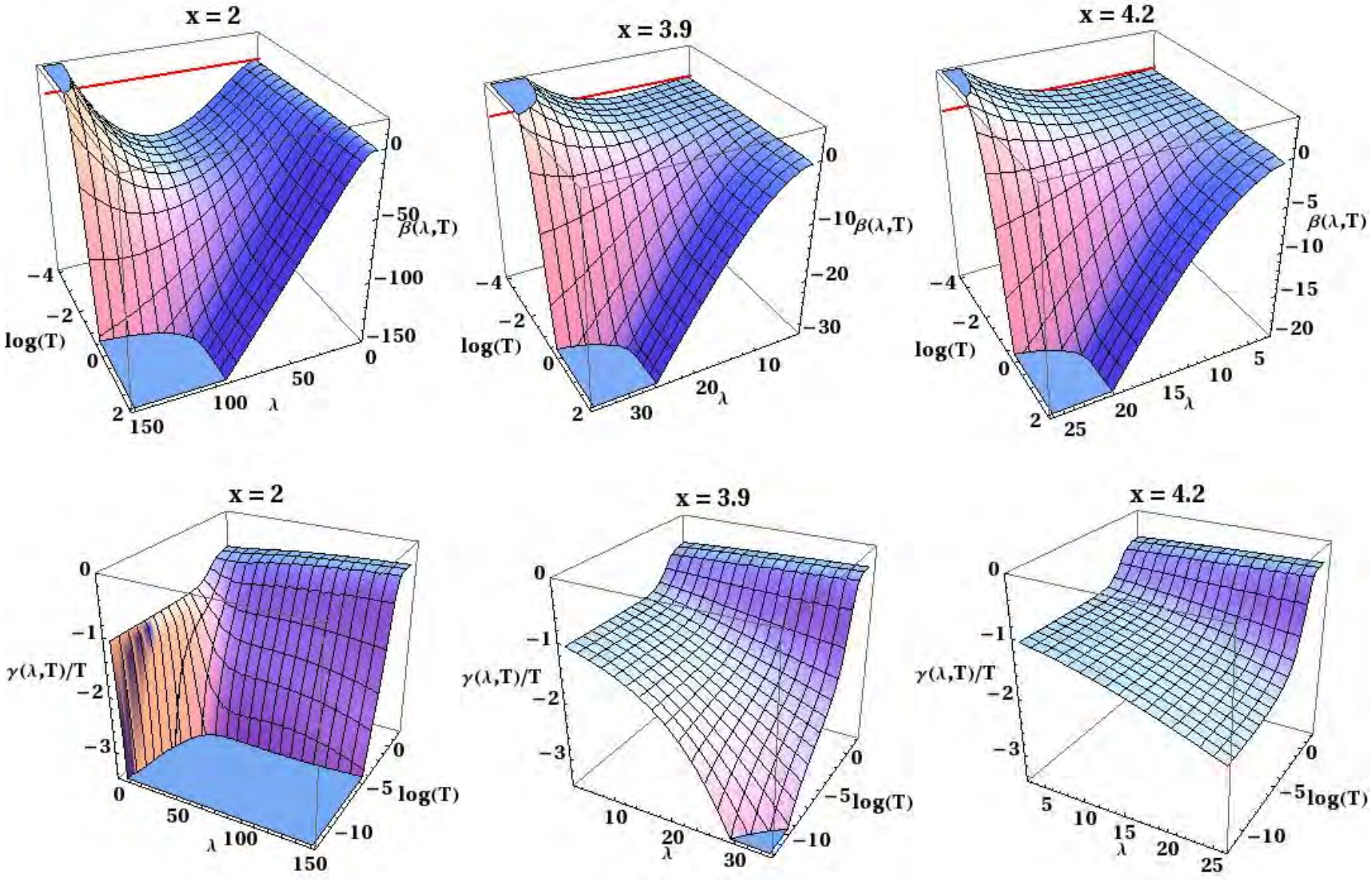

The red lines are added on the top row at $\beta = 0$ in order to show the location of the fixed point.

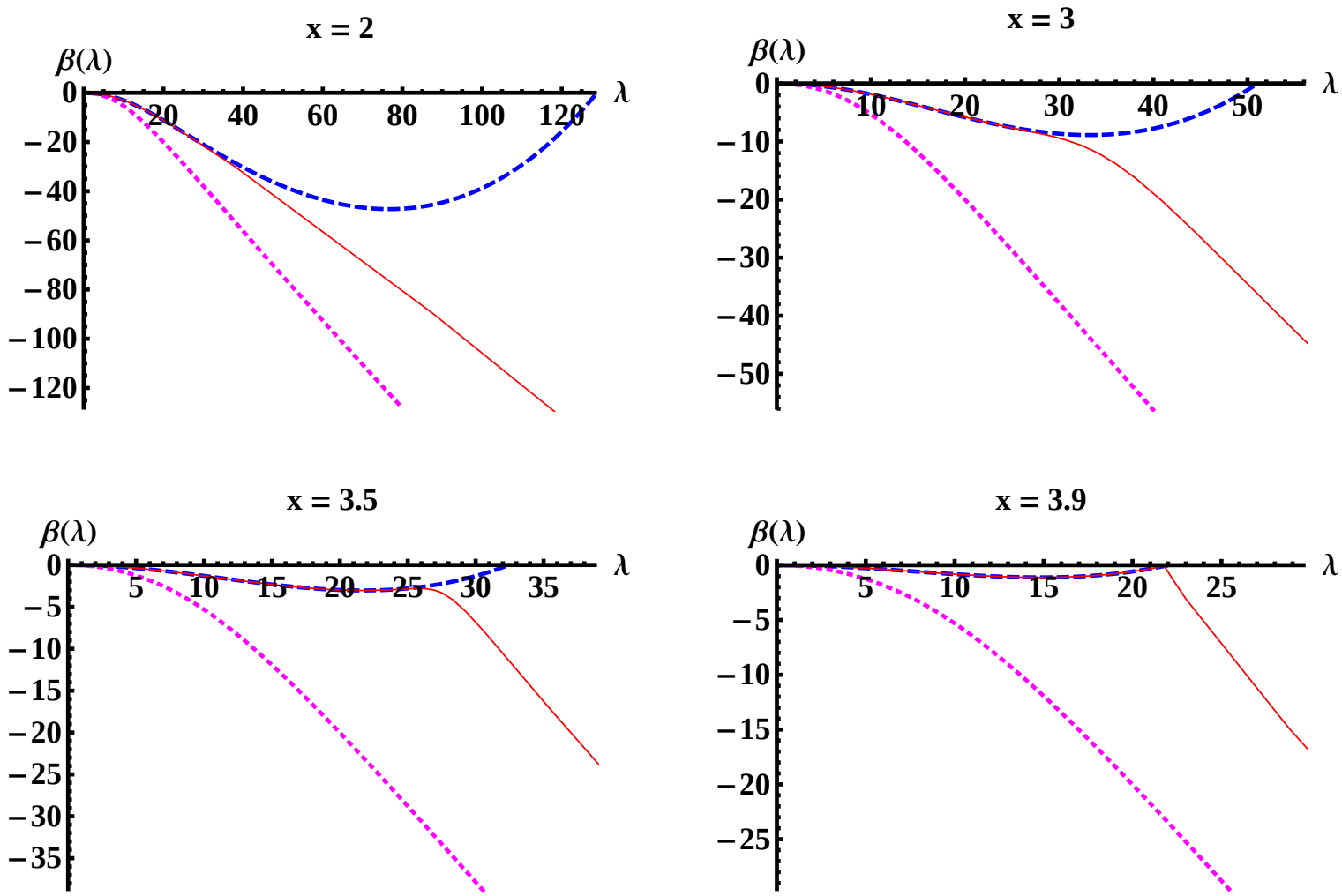

The β-functions for vanishing quark mass for various values of x. The red solid, blue dashed, and magenta dotted curves are the β-functions corresponding to the full numerical solution ($d\lambda/dA$) along the RG flow, the potential $V_{\text{eff}} = V_g - xV_{f0}$, and the potential V_g, respectively.

UV mass vs T_0 and r_1

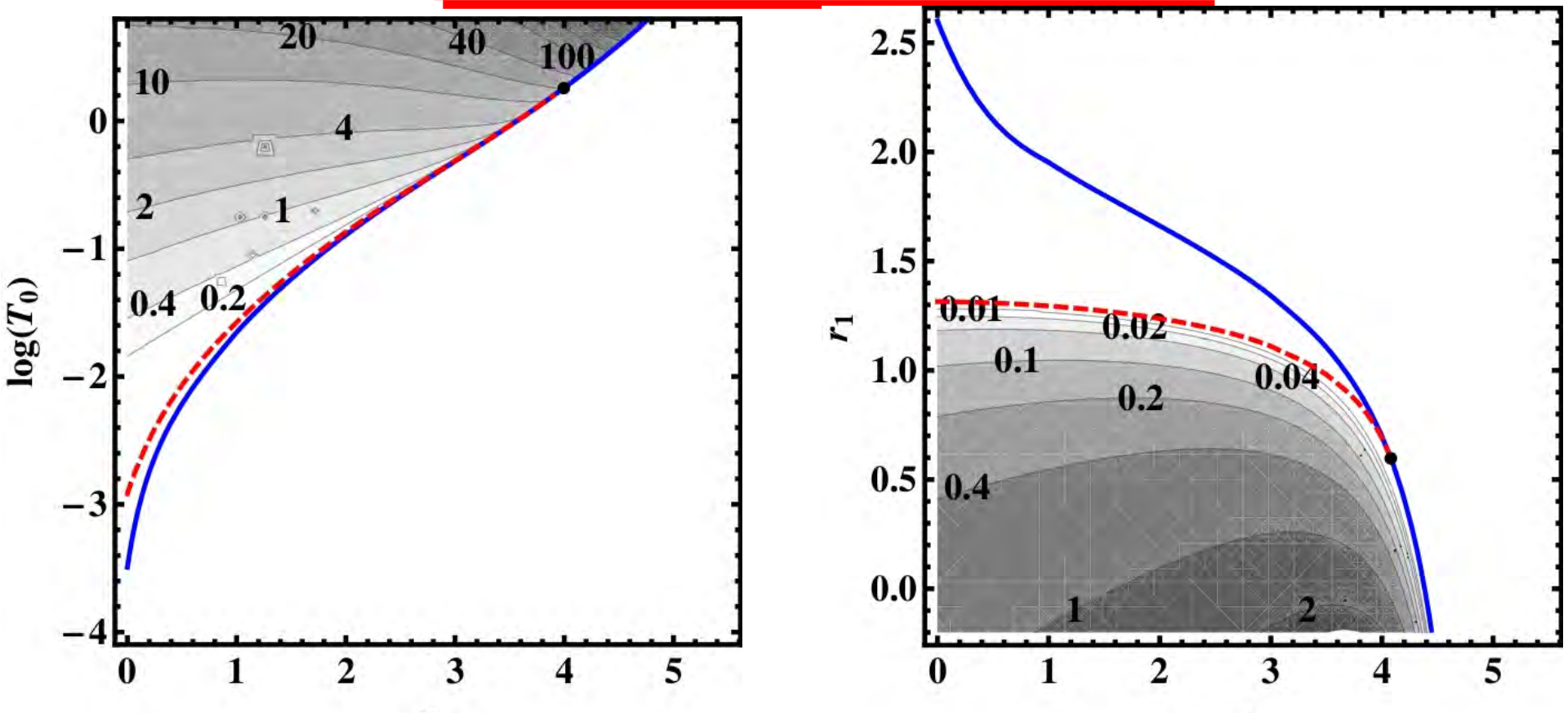

The UV behavior of the background solutions with good IR singularity for the scenario I (left) and parameter T_0 and scenario II (right) and parameter r_1.

The thick blue curve represents a change in the UV behavior, the red dashed curve has zero quark mass, and the contours give the quark mass. The black dot where the zero mass curve terminates lies at the critical value $x = x_c$. For scenario I (II) we have $x_c \simeq 3.9959$ ($x_c \simeq 4.0797$).

Numerical solutions: $T = 0$

$T \equiv 0$ backgrounds (color codes λ, A)

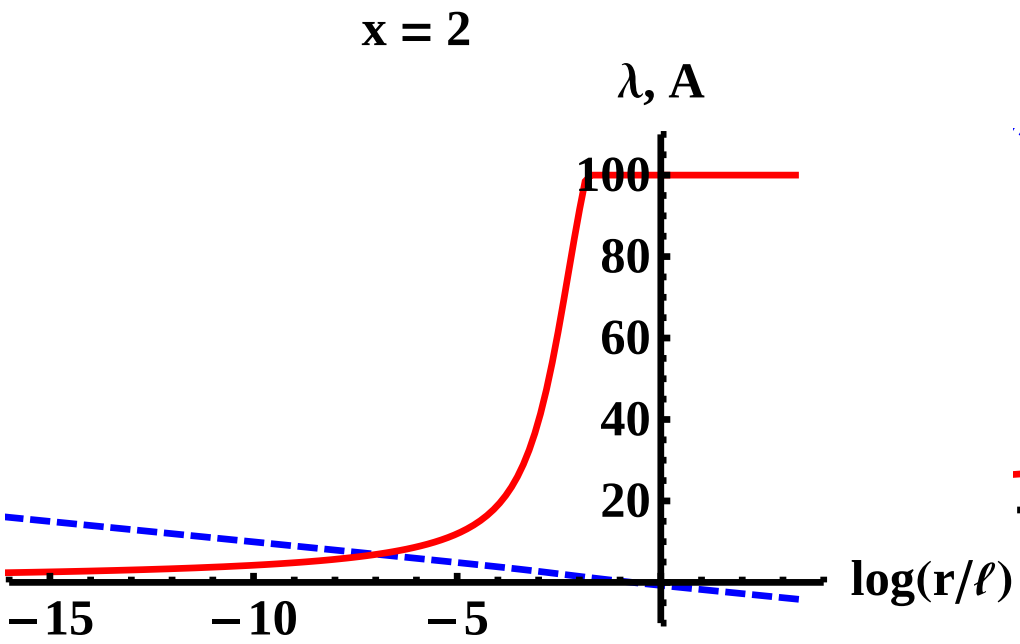

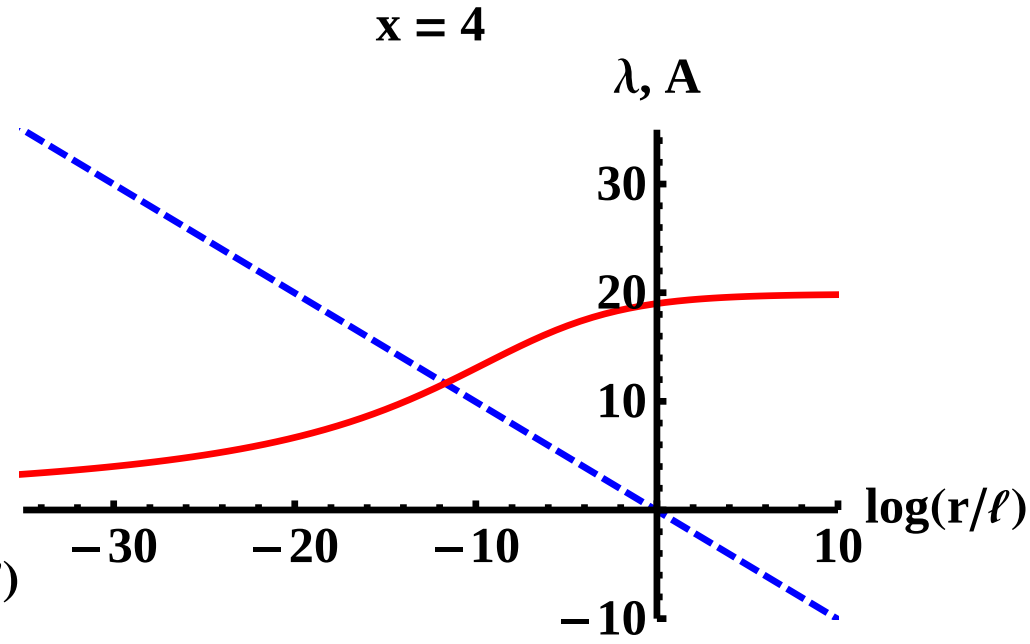

Numerical solutions: Massless with $x < x_c$

Massless backgrounds with $x < x_c \simeq 3.9959$ (λ, A, T)

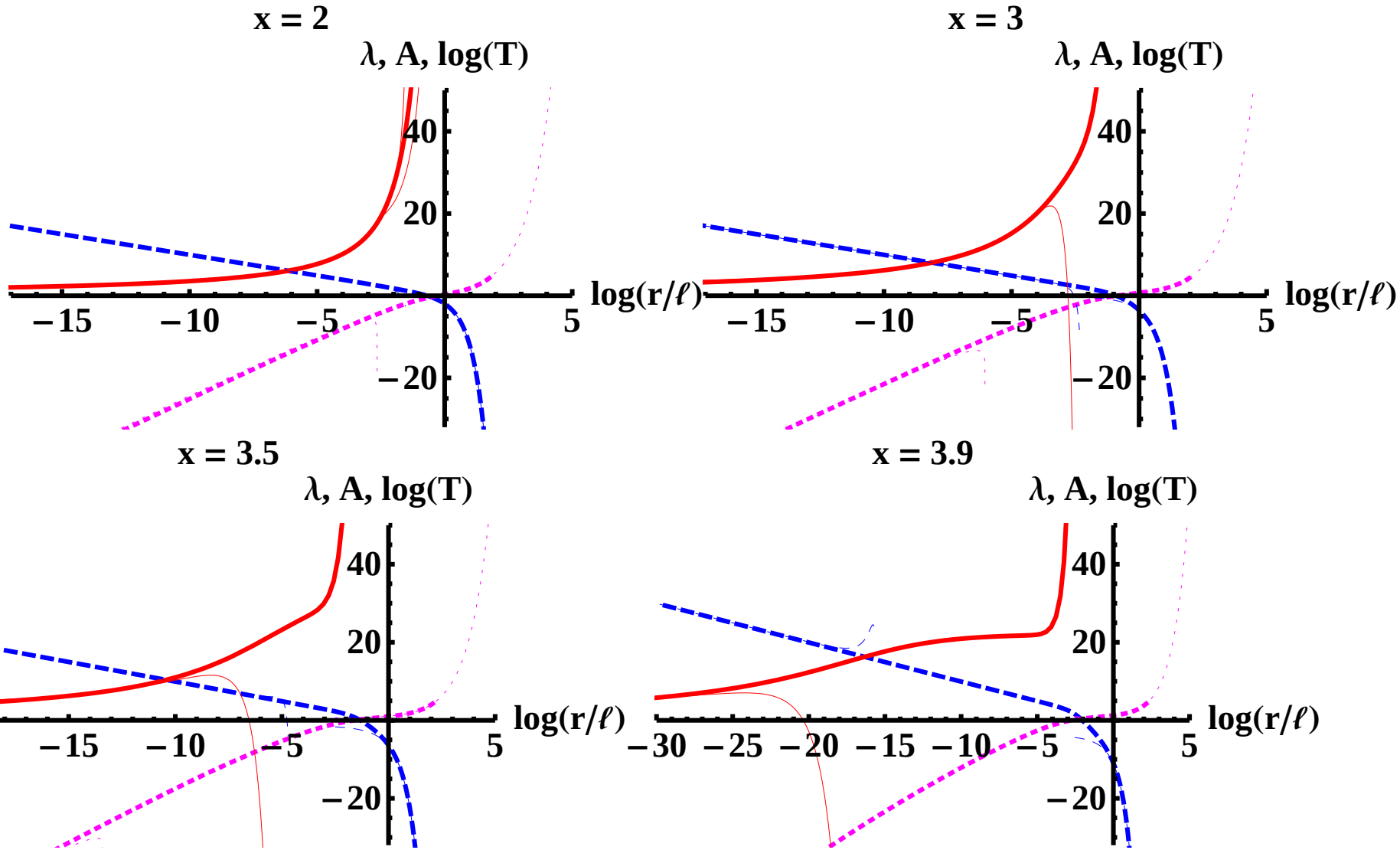

Massless backgrounds: beta functions $\beta = \frac{d\lambda}{dA}$, ($x_c \simeq 3.9959$)

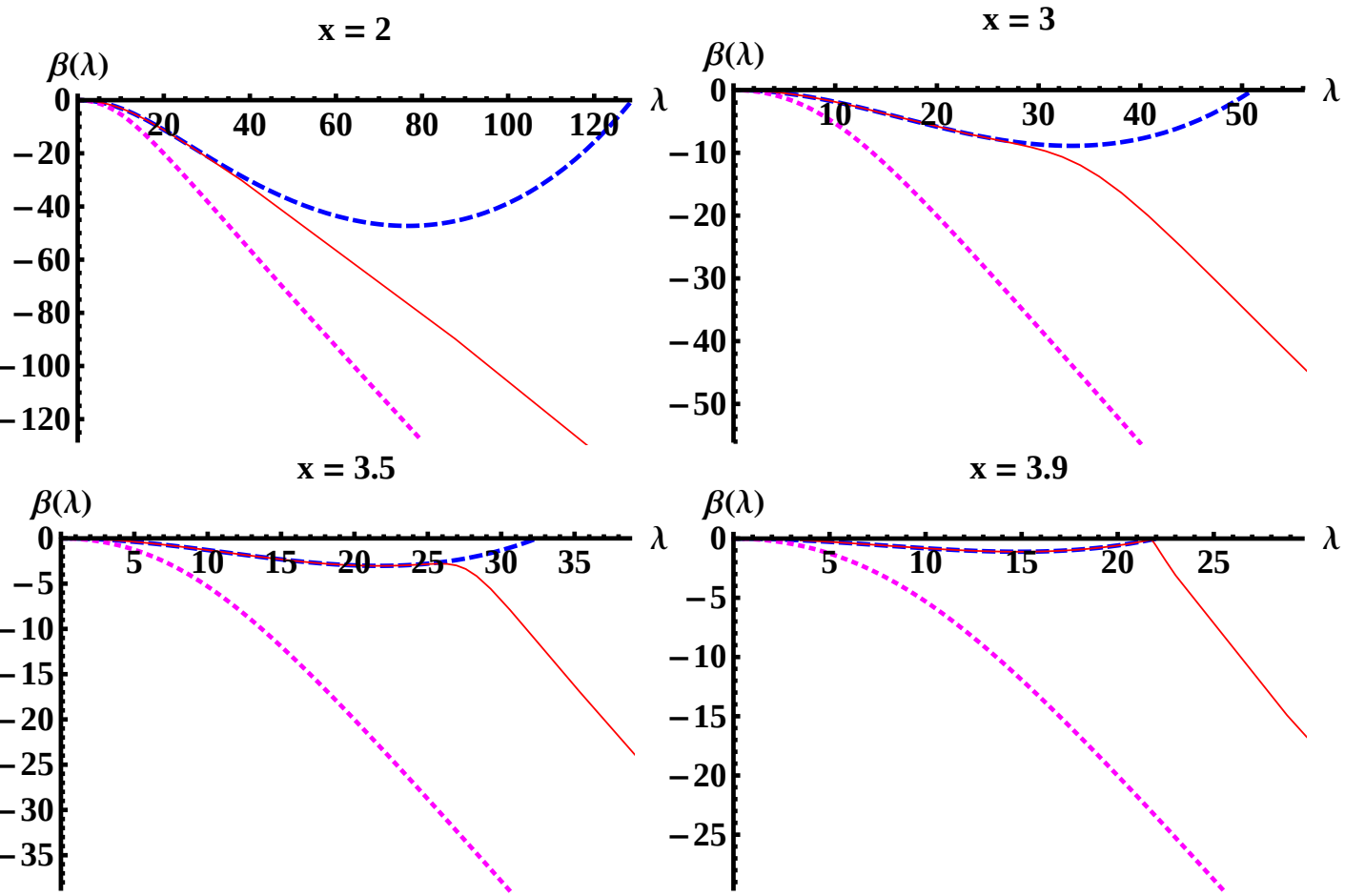

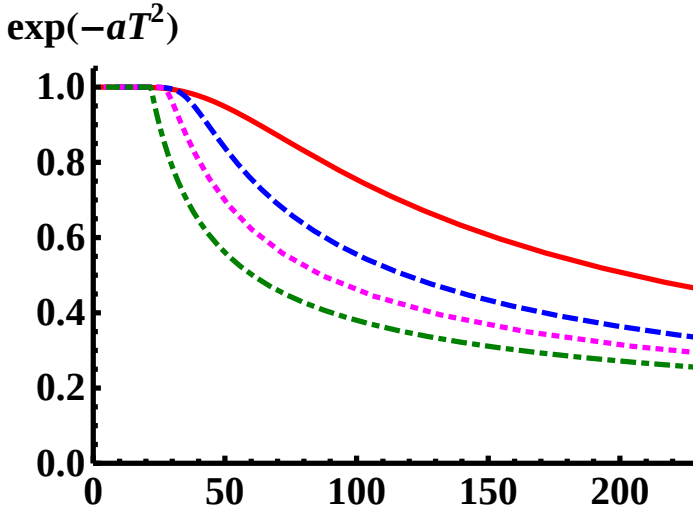

$x = 2, 3, 3.5, 3.9$

.

Massless backgrounds: gamma functions $\frac{\gamma}{T} = \frac{d \log T}{dA}$

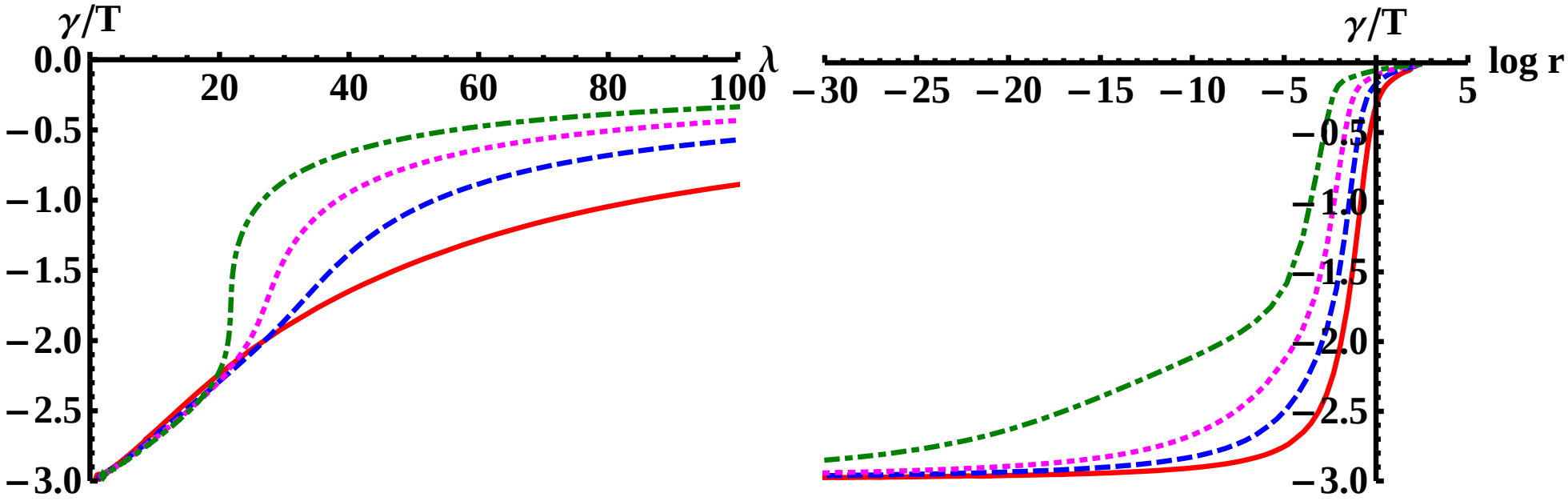

$x = 2, 3, 3.5, 3.9$

Matching to QCD: IR

• In the IR, the tachyon has to diverge $\Rightarrow$ the tachyon action $\propto e^{-T^2}$ becomes small

♠ $V_g(\lambda) \simeq \lambda^{\frac{4}{3}}\sqrt{\lambda}$ chosen as for Yang-Mills, so that a "good" IR singularity exists etc.

♠ $V_0(\lambda)$, $a(\lambda)$, and $h(\lambda)$ chosen to produce tachyon divergence: there are several possibilities.

♠ The phase structure is essentially independent of IR choices.

Choice I:

$$V_g(\lambda) = 12 + \frac{44}{9\pi^2}\lambda + \frac{4619}{3888\pi^4}\frac{\lambda^2}{(1+\lambda/(8\pi^2))^{2/3}}\sqrt{1+\log(1+\lambda/(8\pi^2))}$$

$$V_f(\lambda, T) = V_0(\lambda)e^{-a(\lambda)T^2}$$

$$V_0(\lambda) = \frac{12}{11} + \frac{4(33-2x)}{99\pi^2}\lambda + \frac{23473 - 2726x + 92x^2}{42768\pi^4}\lambda^2$$

$$a(\lambda) = \frac{3}{22}(11-x)$$

$$h(\lambda) = \frac{1}{\left(1+\frac{115-16x}{288\pi^2}\lambda\right)^{4/3}}$$

For which in the IR

$$T(r) \sim T_0 \exp\left[\frac{81\ 3^{5/6}(115-16x)^{4/3}(11-x)}{812944\ 2^{1/6}}\frac{r}{R}\right] \quad , \quad r \to \infty$$

R is the IR scale of the solution. T_0 is the control parameter of the UV mass.

Choice II:

$$a(\lambda) = \frac{3}{22}(11-x)\frac{1+\frac{115-16x}{216\pi^2}\lambda+\frac{\lambda^2}{\lambda_0^2}}{(1+\lambda/\lambda_0)^{4/3}}$$

$$h(\lambda) = \frac{1}{(1+\lambda/\lambda_0)^{4/3}}$$

for which in the IR

$$T(r) \sim \frac{27\ 2^{3/4}3^{1/4}}{\sqrt{4619}}\sqrt{\frac{r-r_1}{R}} \quad , \quad r \to \infty$$

R is the IR scale of the solution. r_1 is the control parameter of the UV mass.

Comparison to previous "guesses"

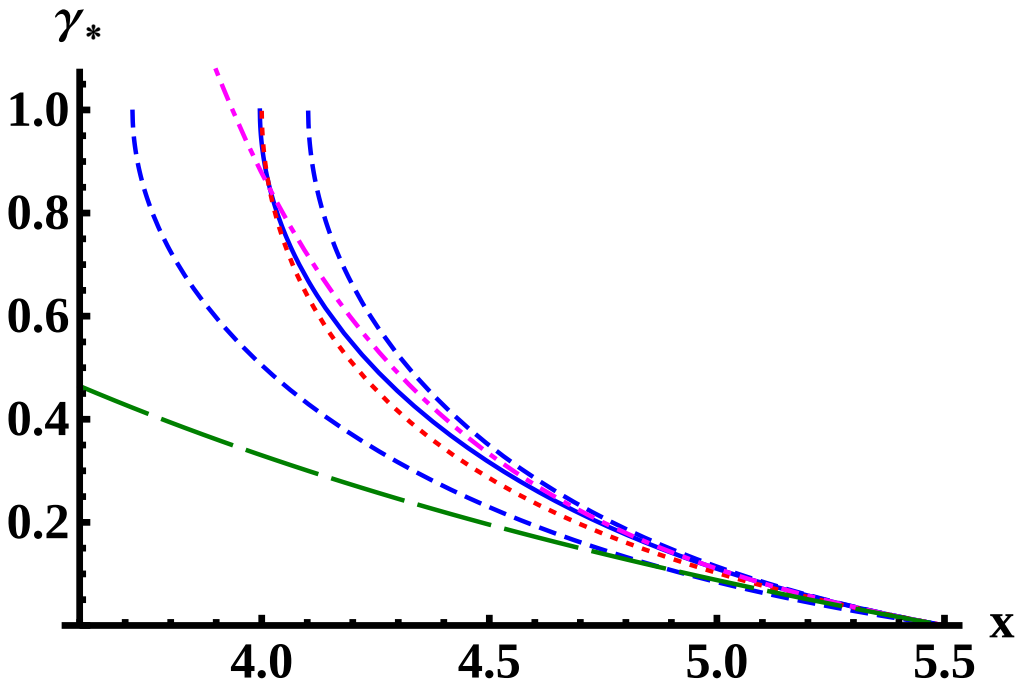

The anomalous dimension of the quark mass at the IR fixed point as a function of x within the conformal window in various approaches.

The solid blue curve is our result for the potential I.

The dashed blue lines show the maximal change as W_0 is varied from 0 (upper curve) to 24/11 (lower curve).

The dotted red curve is the result from a Dyson-Schwinger analysis, the dot-dashed magenta curve is the prediction of two-loop perturbative QCD, and the long-dashed green curve is based on an all-orders β-function.

Miransky scaling for the masses

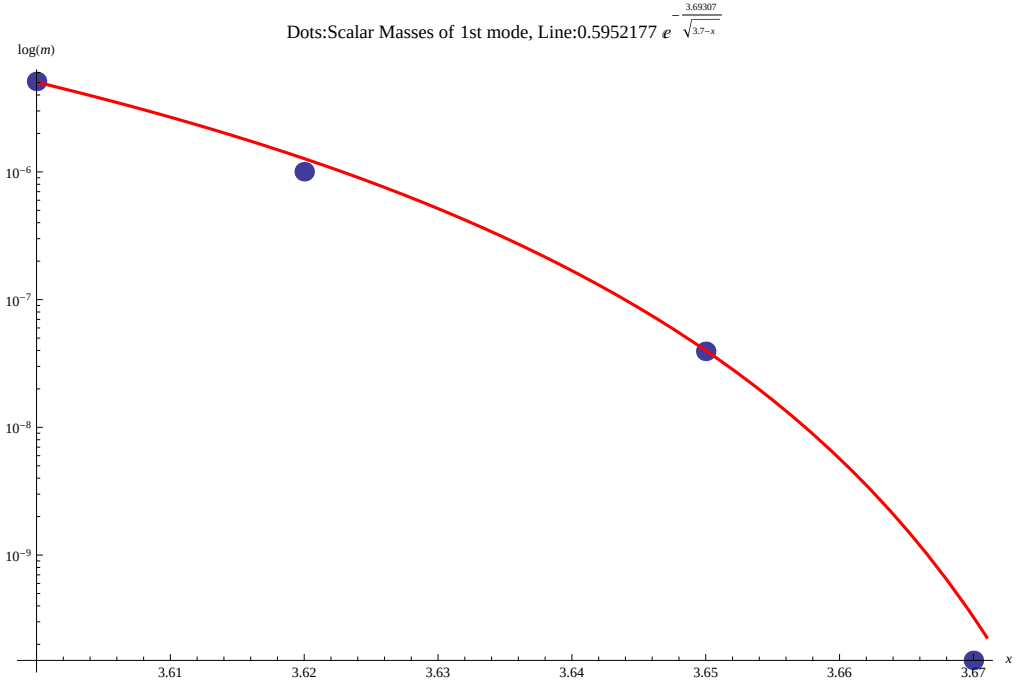

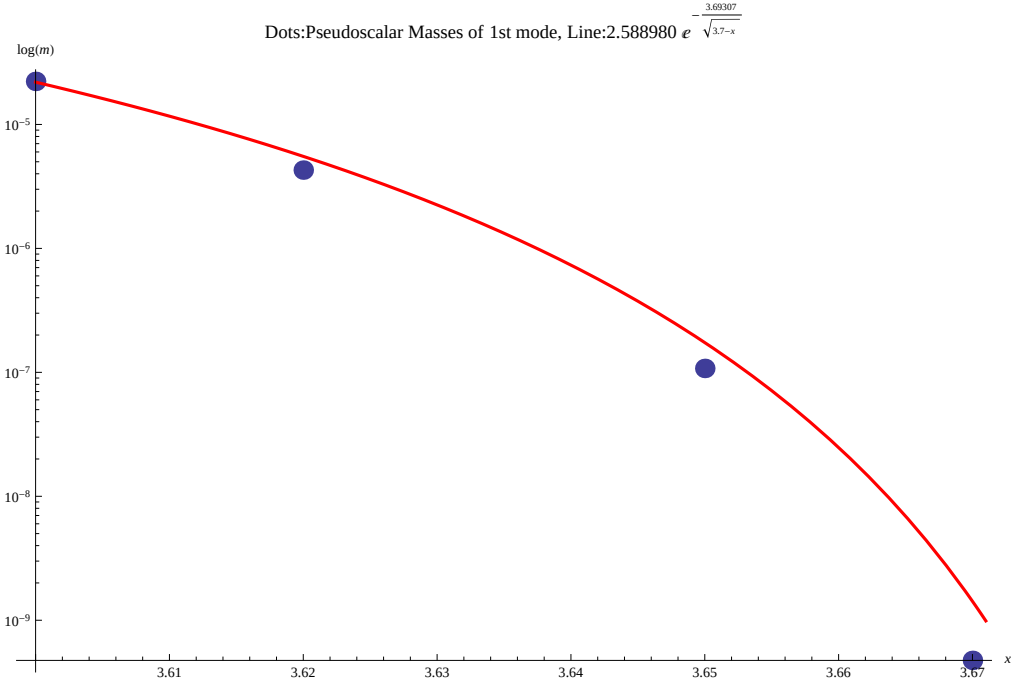

The plots depict the scalar and pseudoscalar masses of the first mode close to x_c fit to the Miransky exponential factor.

RETURN

The holographic models: flavor

- Fundamental quarks arise from $D4$-$\bar{D}4$ branes in 5-dimensions.

$$D4-D4 \quad \text{strings} \quad \rightarrow \quad A_\mu^L \quad \leftrightarrow \quad J_\mu^L = \bar{\psi}_L \sigma_\mu \psi_L$$

$$\overline{D4}-\overline{D4} \quad \text{strings} \quad \rightarrow \quad A_\mu^R \quad \leftrightarrow \quad J_\mu^R = \bar{\psi}_R \bar{\sigma}_\mu \psi_R$$

$$D4-\overline{D4} \quad \text{strings} \quad \rightarrow \quad T \quad \leftrightarrow \quad \bar{\psi}_L \psi_R$$

- For the vacuum structure only the tachyon is relevant.

- An action for the tachyon motivated by the Sen action has been advocated as the proper dynamics of the chiral condensate, giving in general all the expected features of χSB.

Casero+Kiritsis+Paredes

$$\mathcal{S}_{\text{TDBI}} = -N_f N_c M^3 \int d^5x \; V_f(T) \; e^{-\phi} \sqrt{-\det(g_{ab} + \partial_a T \partial_b T)}$$

- It has been tested in a 6d asymptotically-AdS confining background (with constant dilaton) due to Kuperstein+Sonneschein.

Iatrakis+Kiritsis+Paredes

It was shown to have the following properties:

- Confining asymptotics of the geometry trigger chiral symmetry breaking.

- A Gell-Mann-Oakes-Renner relation is generically satisfied.

- The Sen DBI tachyon action with $V \sim e^{-T^2}$ asymptotics induces linear Regge trajectories for mesons.

- The Wess-Zumino (WZ) terms of the tachyon action, computed in string theory, produce the appropriate flavor anomalies, include the axial $U(1)$ anomaly and η'-mixing, and implement a holographic version of the Coleman-Witten theorem.

- The dynamics determines the chiral condensate uniquely a s function of the bare quark mass.

- The mass of the ρ-meson grows with increasing quark mass.

- By adjusting the same parameters as in QCD ($\Lambda_{\rm QCD}$, m_{ud}) a good fit can be obtained of the light meson masses.

The chiral vacuum structure

- We take the potential to be the flat space one

$$V = V_0 \; e^{-T^2}$$

with a maximum at $T = 0$ and a minimum at $T = \infty$.

- Near the boundary $z = 0$, the solution can be expanded in terms of two integration constants as:

$$\tau = c_1 z + \frac{\pi}{6} c_1^3 z^3 \log z + c_3 z^3 + \mathcal{O}(z^5)$$

- c_1, c_3 are related to the quark mass and condensate.

- At the tip of the cigar, the generic behavior of solutions is

$$\tau \sim constant_1 + constant_2 \sqrt{z - z_\Lambda}$$

- With special tuned condition there is a one-parameter family of diverging solutions in the IR depending on a single parameter:

$$\tau = \frac{C}{(z_\Lambda - z)^{\frac{3}{20}}} - \frac{13}{6\pi C} (z_\Lambda - z)^{\frac{3}{20}} + \dots$$

• This is the correct "regularity condition" in the IR as τ is allowed to diverge only at the tip.

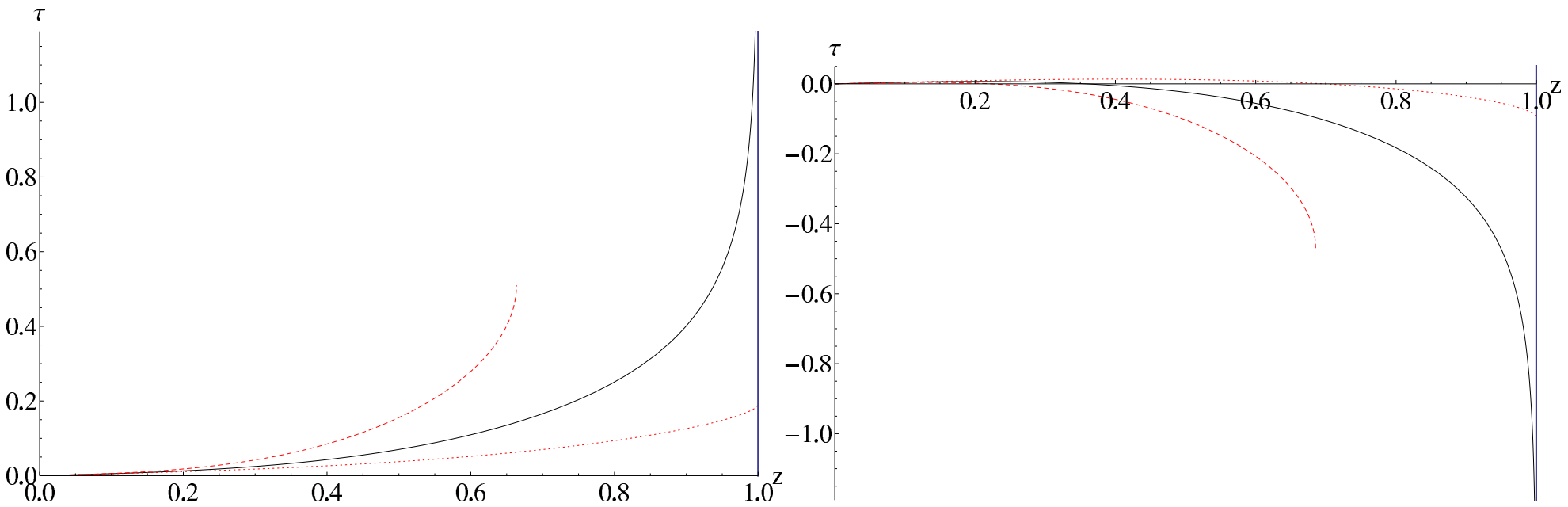

All the graphs are plotted using $z_\Lambda = 1$, $\mu^2 = \pi$ and $c_1 = 0.05$. The tip of the cigar is at $z = z_\Lambda = 1$. On the left, the solid black line represents a solution with $c_3 \approx 0.3579$ for which τ diverges at z_Λ. The red dashed line has a too large c_3 ($c_3 = 1$) - such that there is a singularity at $z = z_s$ where $\partial_z \tau$ diverges while τ stays finite. This is unacceptable since the solution stops at $z = z_s$ where the energy density of the flavor branes diverges. The red dotted line corresponds to $c_3 = 0.1$; this kind of solution is discarded because the tachyon stays finite everywhere. The plot in the right is done with the same conventions but with negative values of $c_3 = -0.1, -0.3893, -1$. For $c_3 \approx -0.3893$ there is a solution of the differential equation such that τ diverges to $-\infty$. This solution is unstable.

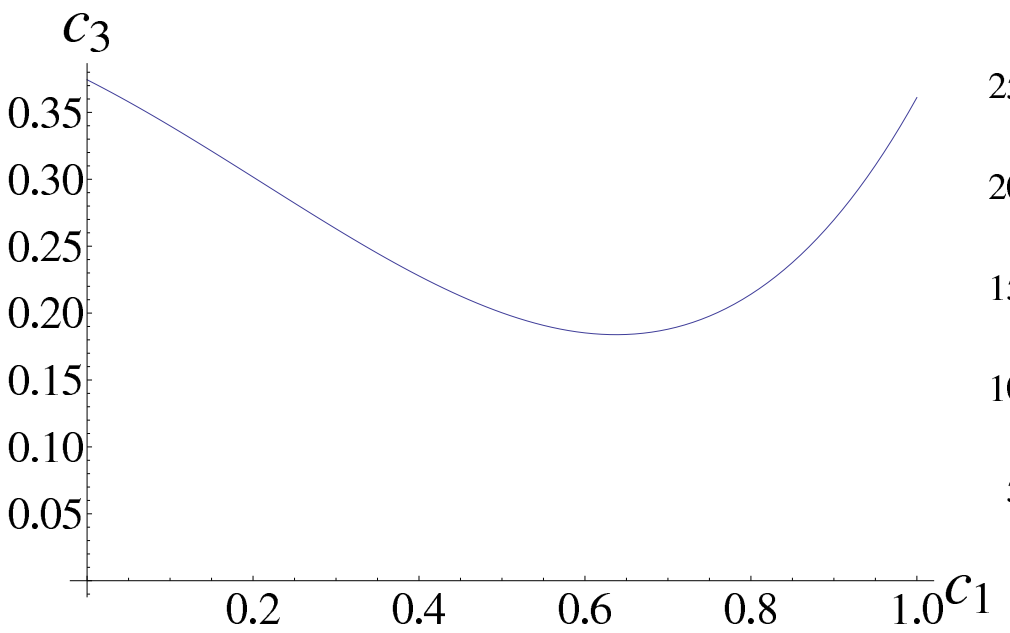

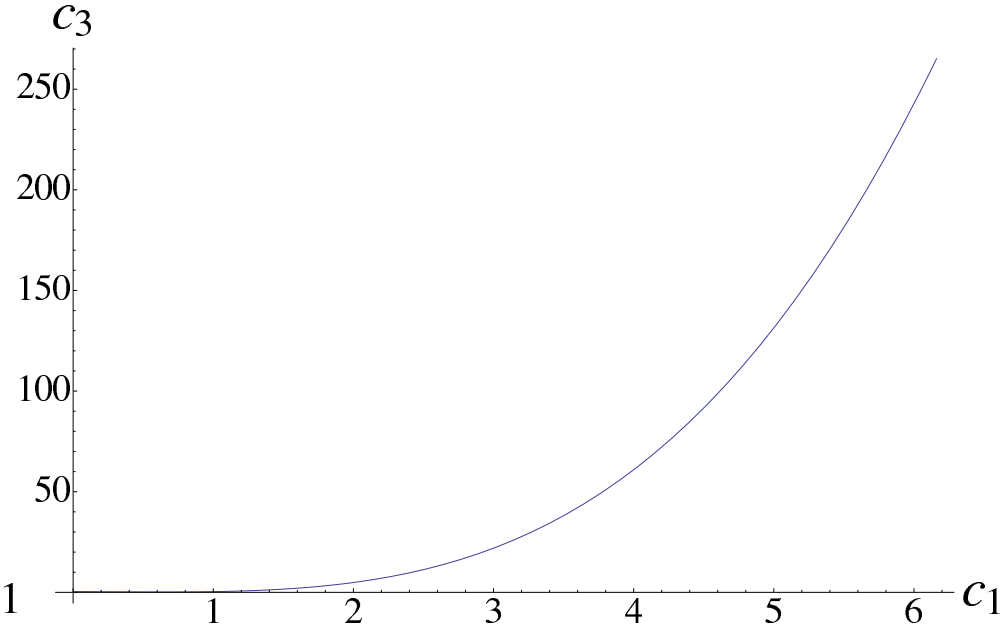

- Chiral symmetry breaking is manifest.

Chiral restauration at deconfinement

- In the deconfined phase, the bulk metric is that of a bh.

- The branes now are allowed to enter the horizon without recombining.

- To avoid intermediate singularities of the solution the boundary conditions must be tuned so that tachyon is finite at the horizon.

- Near the horizon the correct solution behaves as a one-parameter family

$$\tau = c_T - \frac{3c_T}{5z_T}(z_T - z) - \frac{9c_T}{200z_T}(8 + \mu^2 {c_T}^2)(z_T - z)^2 + \dots$$

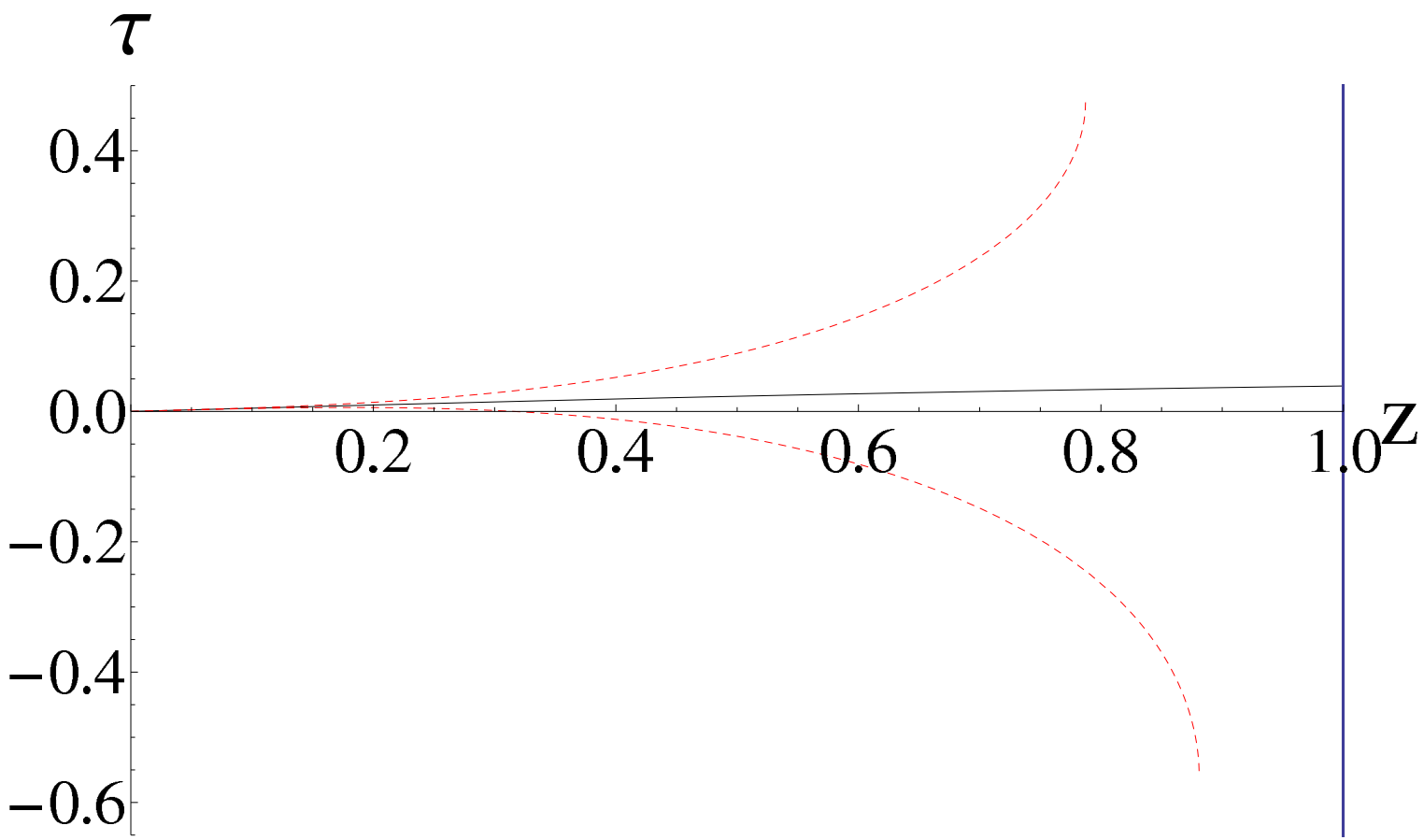

Plots corresponding to the deconfined phase. We have taken $c_1 = 0.05$. The solid line displays the physical solution $c_3 = -0.0143$ whereas the dashed lines ($c_3 = -0.5$ and $c_3 = 0.5$) are unphysical and end with a behavior of the type $\tau = k_1 - k_2\sqrt{z_s - z}$.

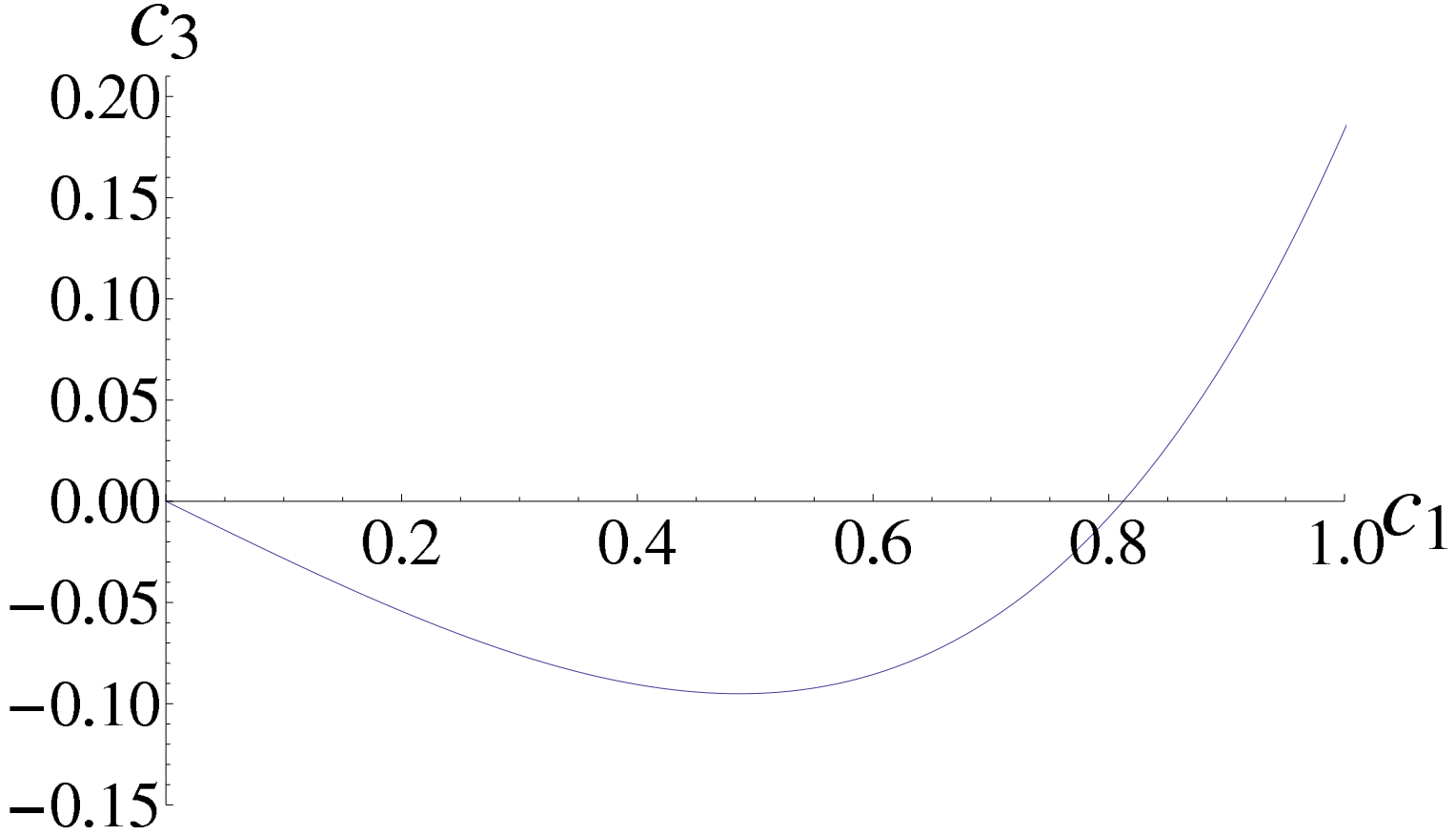

These plots give the values of c_3 determined numerically by demanding the correct IR behavior of the solution, as a function of c_1.

Jump of the condensate at the phase transition

- From holographic renormalization we obtain

$$\langle \bar{q}q \rangle = \frac{1}{\beta}(2\pi\alpha' \mathcal{K} R^3 \lambda) \left(-4c_3 + \left(\frac{m_q}{\beta}\right)^3 \mu^2 (1+\alpha) \right) \quad , \quad m_q = \beta \; c_1$$

- We calculate the jump at the phase transition that is scheme independent for a fixed quark mass.

$$\Delta\langle \bar{q}q \rangle \equiv \langle \bar{q}q \rangle_{conf} - \langle \bar{q}q \rangle_{deconf} = -4\frac{1}{\beta}(2\pi\alpha' \mathcal{K} R^3 \lambda)\Delta c_3$$

- This is equivalent to Δc_3

- We plot it as a function of the quark mass.

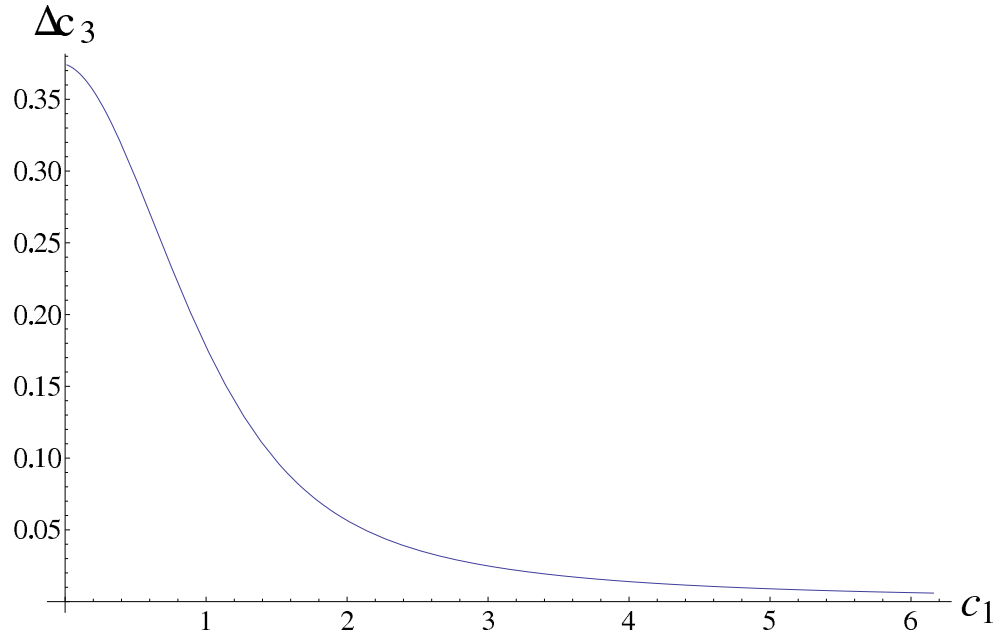

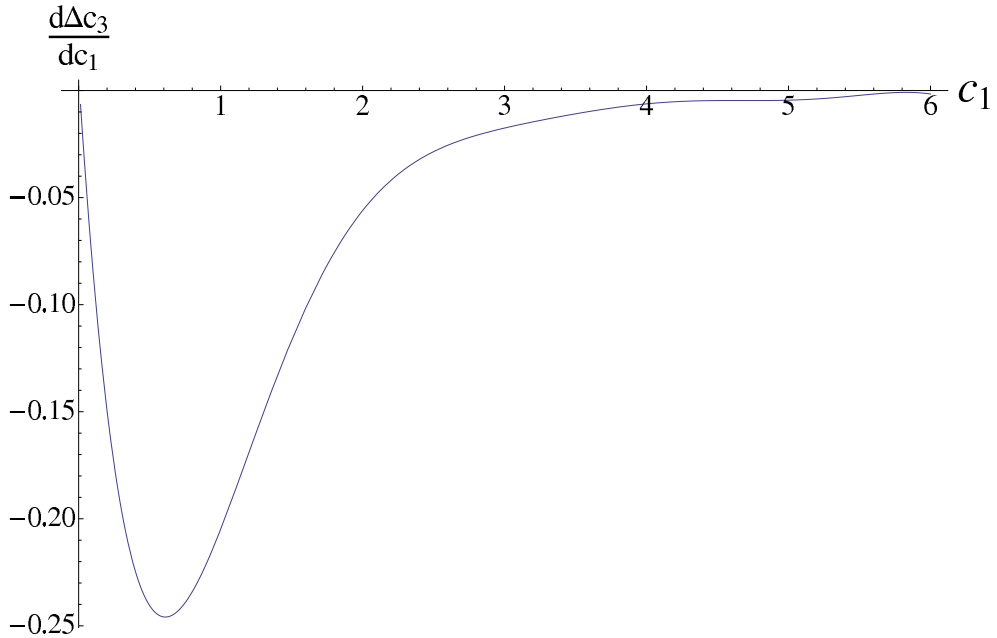

The finite jump of the quark condensate and its derivative with respect to c_1 when the confinement-deconfinement transition takes place. The important features appear when $m_q \sim \Lambda_{QCD}$

Meson spectra

For the vectors

$$z_\Lambda\, m_V^{(1)} = 1.45 + 0.718 c_1\ , \quad z_\Lambda\, m_V^{(2)} = 2.64 + 0.594 c_1\ , \quad z_\Lambda\, m_V^{(3)} = 3.45 + 0.581 c_1\ ,$$
$$z_\Lambda\, m_V^{(4)} = 4.13 + 0.578 c_1\ , \quad z_\Lambda\, m_V^{(5)} = 4.72 + 0.577 c_1\ , \quad z_\Lambda\, m_V^{(6)} = 5.25 + 0.576 c_1\ .$$

For the axial vectors:

$$z_\Lambda\, m_A^{(1)} \approx 2.05 + 1.46 c_1\ , \quad z_\Lambda\, m_A^{(2)} \approx 3.47 + 1.24 c_1\ , \quad z_\Lambda\, m_A^{(3)} \approx 4.54 + 1.17 c_1\ ,$$
$$z_\Lambda\, m_A^{(4)} \approx 5.44 + 1.13 c_1\ , \quad z_\Lambda\, m_A^{(5)} \approx 6.23 + 1.11 c_1\ , \quad z_\Lambda\, m_A^{(6)} \approx 6.95 + 1.10 c_1\ .$$

For the pseudoscalars:

$$z_\Lambda\, m_P^{(1)} \approx \sqrt{3.53 c_1^2 + 6.33 c_1}\ , \quad z_\Lambda\, m_P^{(2)} \approx 2.91 + 1.40 c_1\ , \quad z_\Lambda\, m_P^{(3)} \approx 4.07 + 1.27 c_1\ ,$$
$$z_\Lambda\, m_P^{(4)} \approx 5.04 + 1.21 c_1\ , \quad z_\Lambda\, m_P^{(5)} \approx 5.87 + 1.17 c_1\ , \quad z_\Lambda\, m_P^{(6)} \approx 6.62 + 1.15 c_1\ .$$

For the scalars:

$$z_\Lambda\, m_S^{(1)} = 2.47 + 0.683 c_1\ , \quad z_\Lambda\, m_S^{(2)} = 3.73 + 0.488 c_1\ , \quad z_\Lambda\, m_S^{(3)} = 4.41 + 0.507 c_1\ ,$$
$$z_\Lambda\, m_S^{(4)} = 4.99 + 0.519 c_1\ , \quad z_\Lambda\, m_S^{(5)} = 5.50 + 0.536 c_1\ , \quad z_\Lambda\, m_S^{(6)} = 5.98 + 0.543 c_1\ .$$

- Valid up to $c_1 \sim 1$.
- In qualitative agreement with lattice results

Laerman+Schmidt., Del Debbio+Lucini+Patela+Pica, Bali+Bursa

Mass dependence of f_π

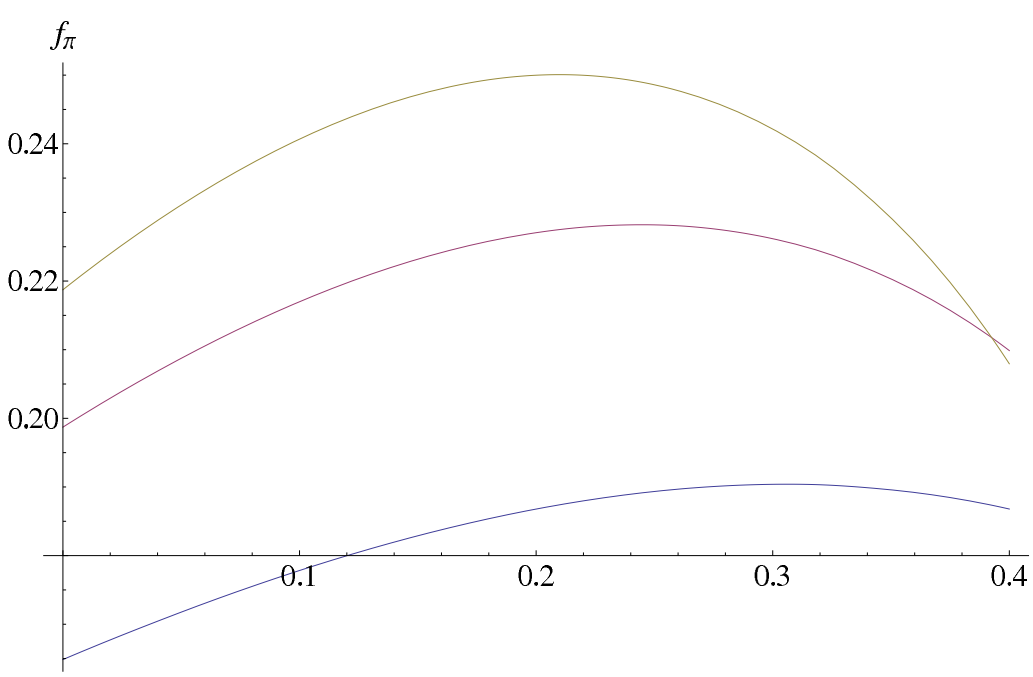

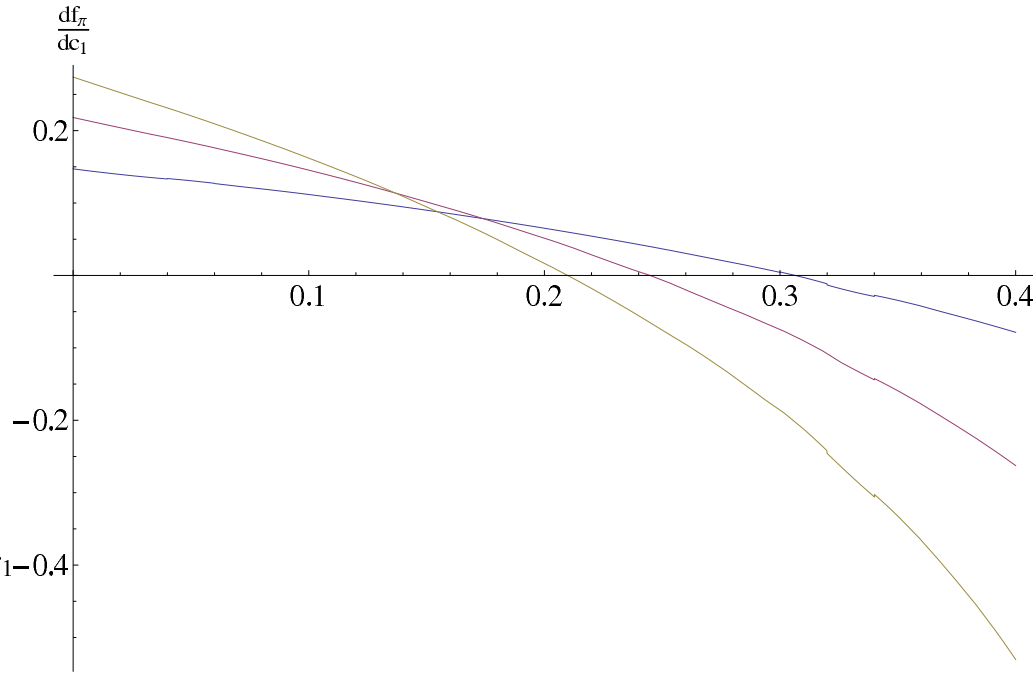

The pion decay constant and its derivative as a function of c_1 - the quark mass. The different lines correspond to different values of k. From bottom to top (on the right plot, from bottom to top in the vertical axis) $k = \frac{12}{\pi^2}, \frac{24}{\pi^2}, \frac{36}{\pi^2}$. The pion decay constant comes in units of z_Λ^{-1}.

Linear Regge Trajectories

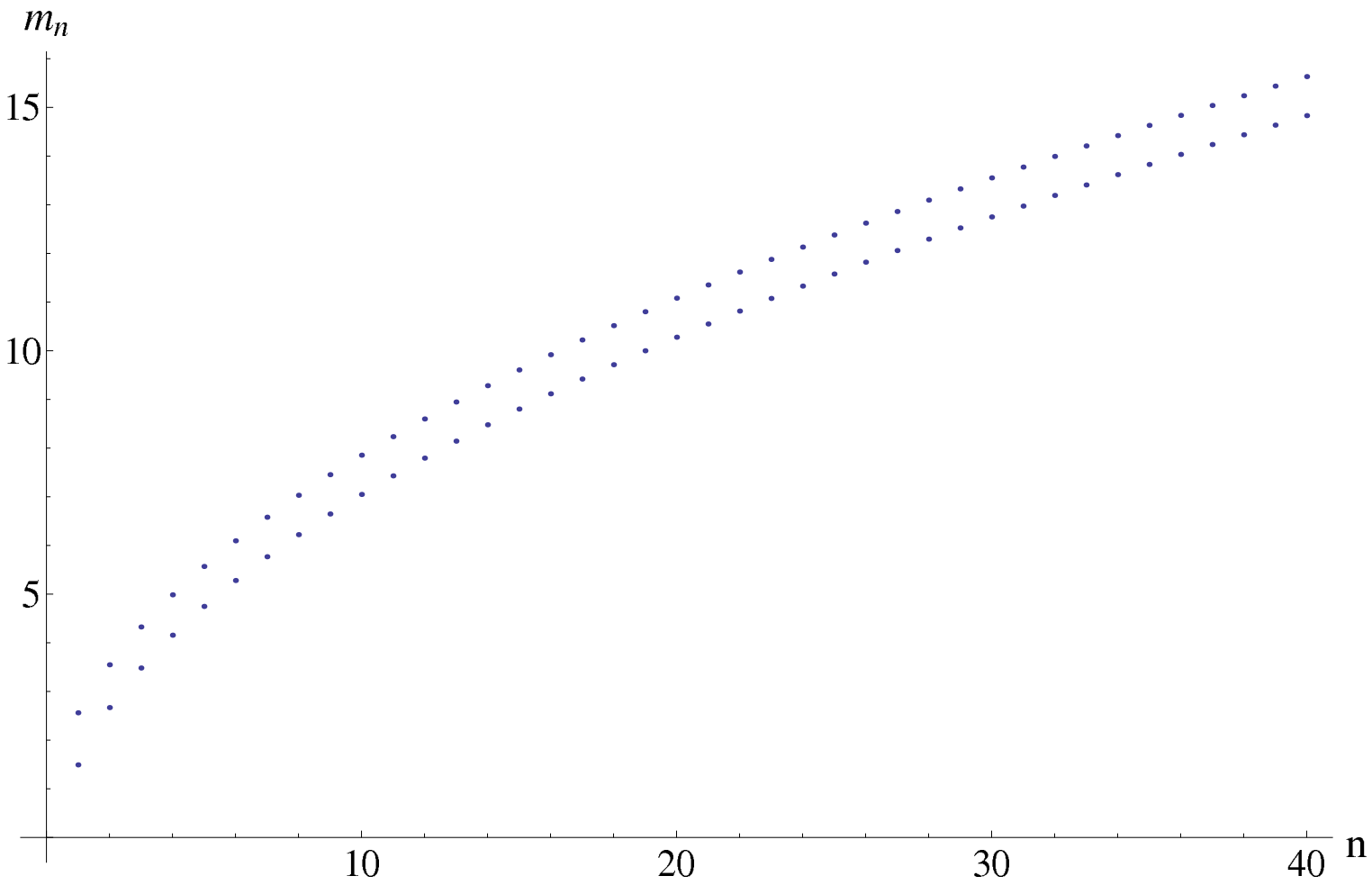

Results corresponding to the forty lightest vector states with $c_1 = 0.05$ and $c_1 = 1.5$.

Walking

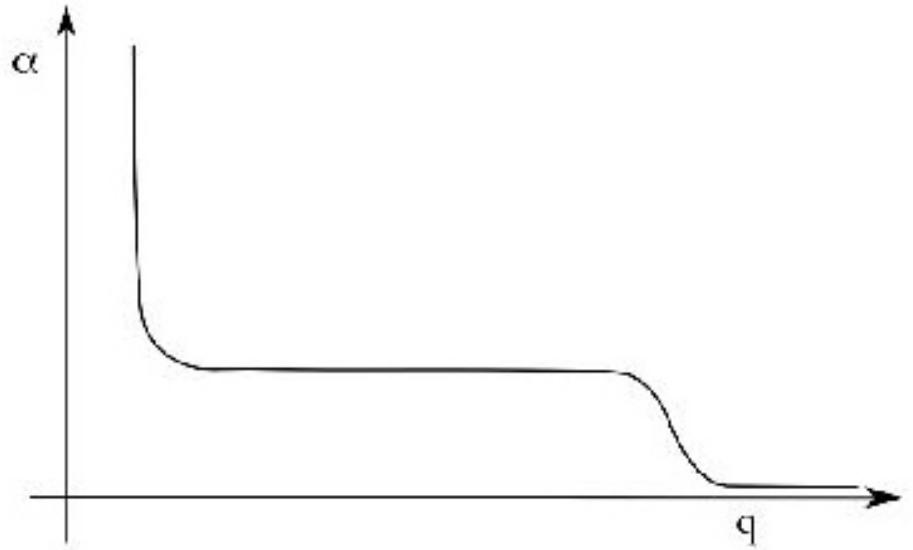

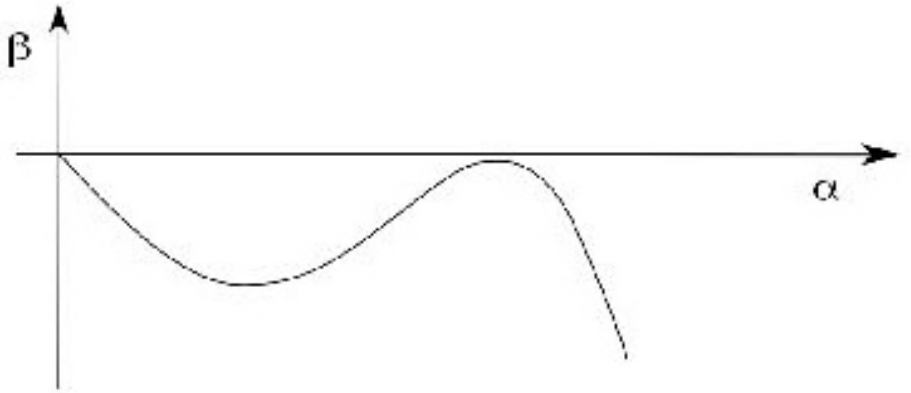

RETURN

The phase diagram

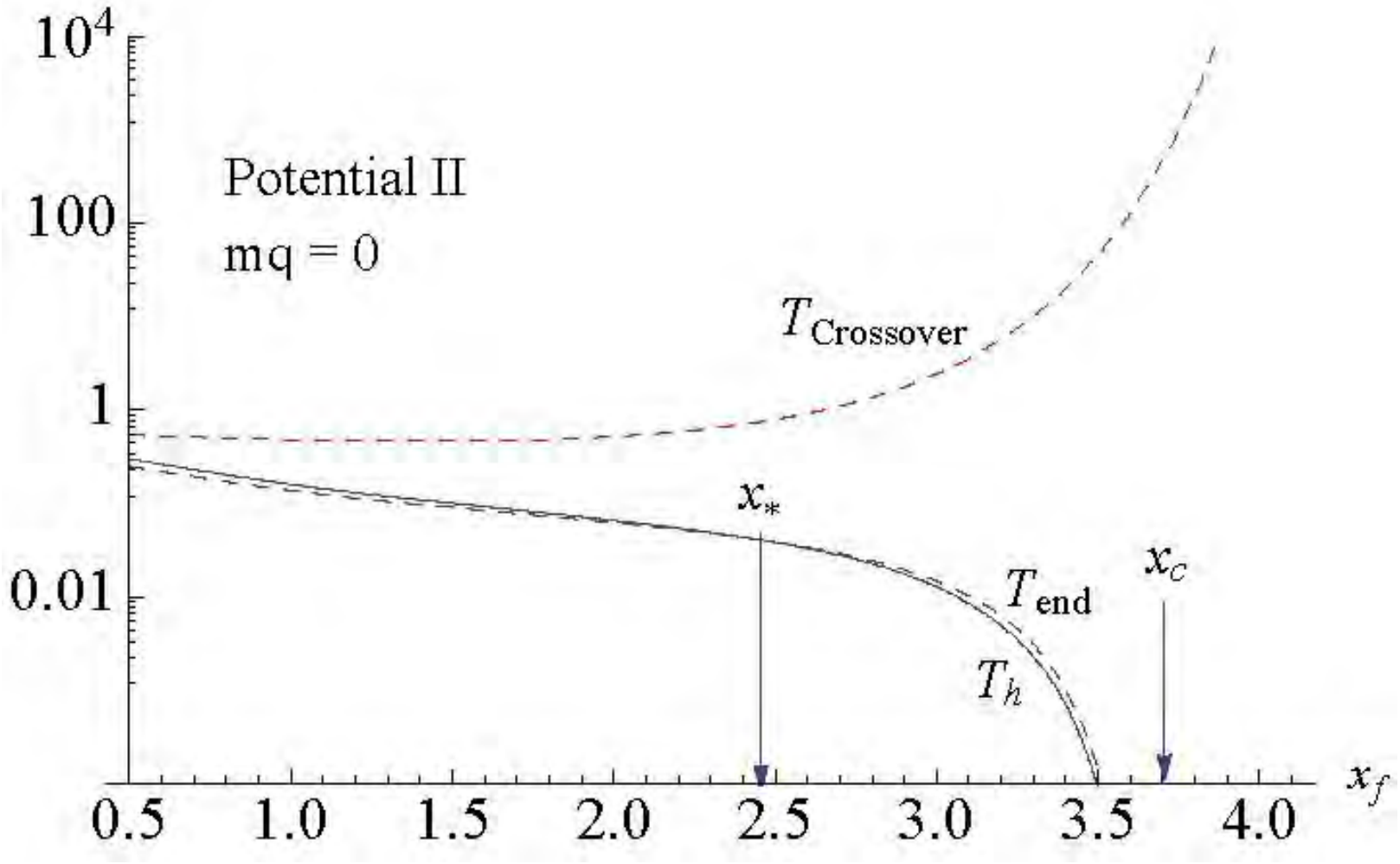

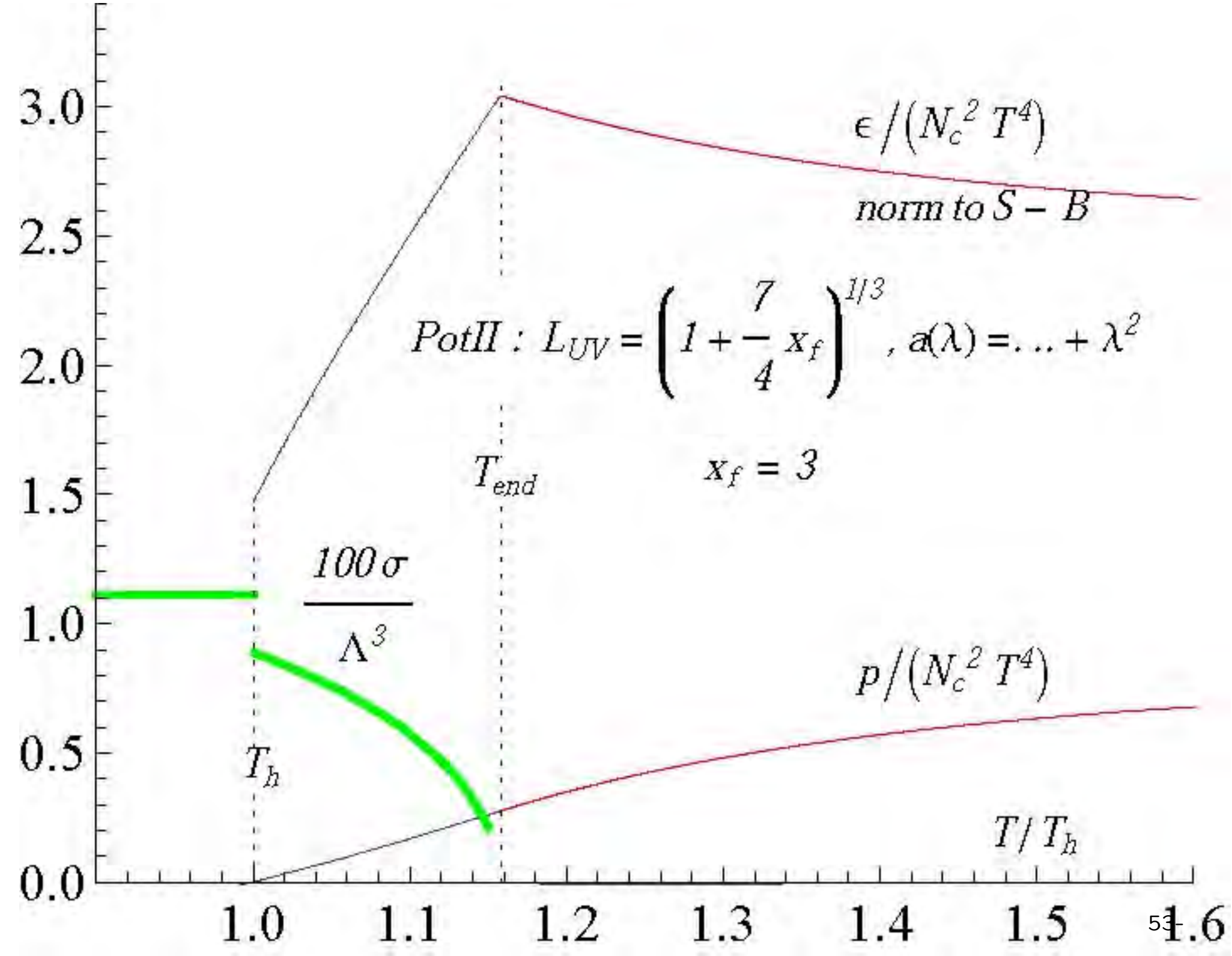
3.0
2.5
2.0
1.5
1.0
0.5
0.0
1.0
1.1
1.2
1.3
1.4
1.5
1.6
$\epsilon/(N_c^2 T^4)$
norm to $S-B$
$PotII: L_{UV} = \left(1 + \frac{7}{4} x_f\right)^{1/3}$, $a(\lambda) = \ldots + \lambda^2$
$x_f = 3$
T_{end}
$\frac{100\sigma}{\Lambda^3}$
T_h
$p/(N_c^2 T^4)$
T/T_h

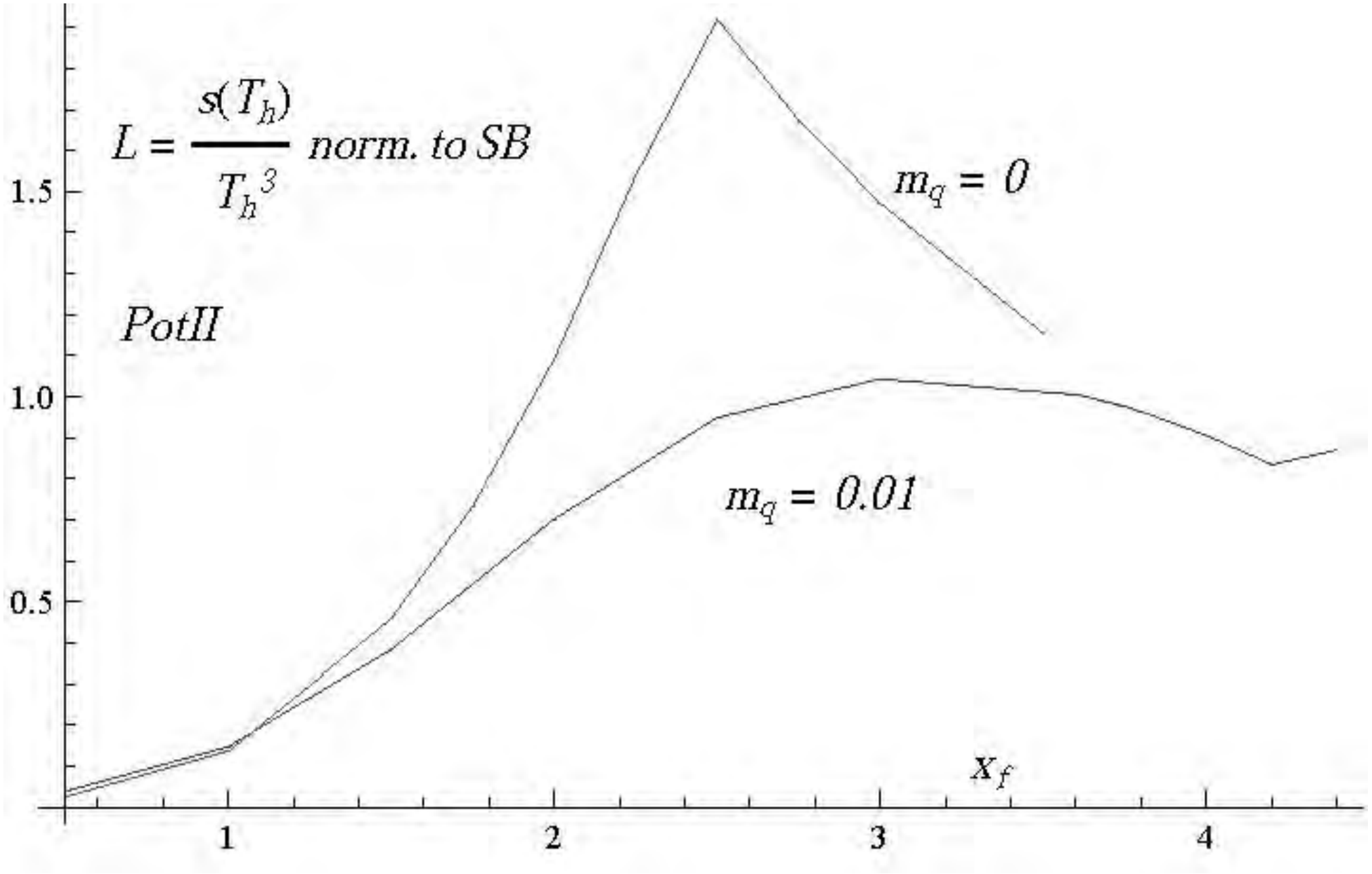
$L = \frac{s(T_h)}{T_h^3}$ norm. to SB
PotII
$m_q = 0$
$m_q = 0.01$
1.5
1.0
0.5
x_f
1
2
3
4

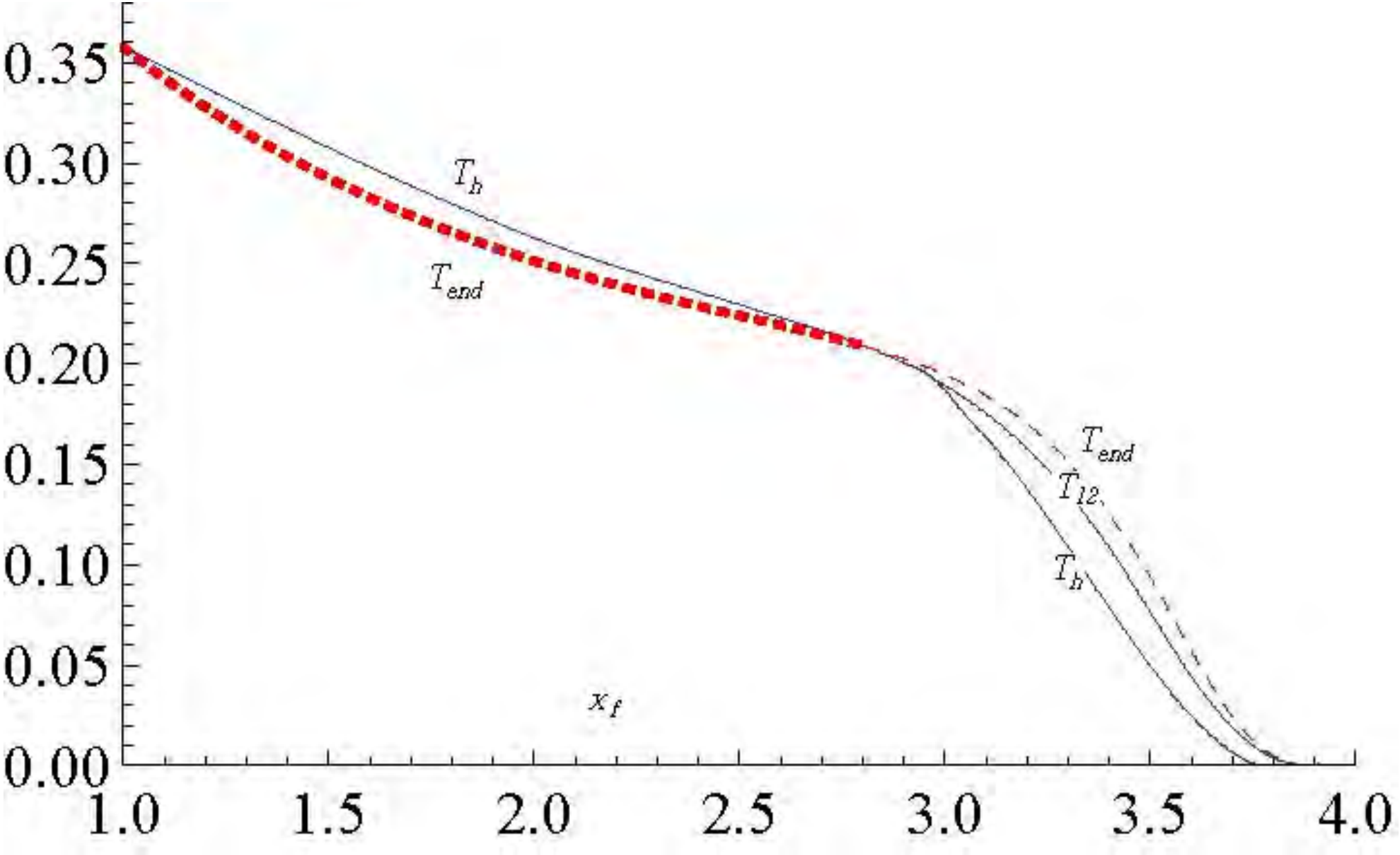
0.35
0.30
0.25
0.20
0.15
0.10
0.05
0.00
1.0
1.5
2.0
2.5
3.0
3.5
4.0
T_h
T_{end}
T_{end}
T_{12}
T_h
x_f

Detailed plan of the presentation

- Title page 0 minutes
- Bibliography 1 minutes
- Introduction 3 minutes
- The Veneziano Limit 5 minutes
- The Banks-Zaks region 7 minutes
- Walking, Technicolor, S-parameter, Dilatons 8 minutes
- Strategy 9 minutes
- The holographic models:glue 12 minutes
- The holographic models:flavor 14 minutes
- Fusion 16 minutes
- Parameters 17 minutes
- The effective potential 19 minutes
- Condensate dimension at the IR fixed point 21 minutes

- UV mass vs IR parameter 25 minutes
- Recap 26 minutes
- Walking 27 minutes
- BKT scaling 29 minutes
- Spectra 32 minutes
- Finite Temperature 34 minutes
- Finite Temperature: The generic phase diagram 36 minutes
- The different black hole solutions 44 minutes
- Finite small mass 45 minutes
- The phase diagrams 47 minutes
- Outlook 48 minutes

- N=1 sQCD 52 minutes
- Walking Region+Technicolor 58 minutes
- Below the BF bound 61 minutes
- Matching to QCD 64 minutes
- Varying the model 66 minutes
- The IR fixed point 67 minutes
- Matching to QCD : UV 68 minutes
- Matching to QCD : IR 71 minutes
- The free energy 73 minutes
- Walking 78 minutes
- Holographic β-functions 81 minutes
- UV mass vs T_0 and r_1 87 minutes
- Numerical solutions :$T = 0$ 89 minutes
- Numerical solutions: Massless with $x < x_c$ 94 minutes
- Matching to QCD 95 minutes

- Comparison to previous guesses 96 minutes
- Miransky scaling for the masses 97 minutes
- The holographic models:flavor 99 minutes
- The chiral vacuum structure 102 minutes
- Chiral restauration at deconfinement 104 minutes
- Jump of the condensate at the phase transition 106 minutes
- Meson Spectra 108 minutes
- Mass dependence of f_π 109 minutes
- Linear Regge trajectories 110 minutes
- Walking 111 minutes
- Phase diagram 112 minutes